Divergent Functional Diversification Patterns in the SEP/AGL6/AP1 MADS-box Transcription Factor Superclade

Patrice Morel, Pierre Chambrier, Véronique Boltz, Sophy Chamot, Frédérique Rozier, Suzanne Rodrigues Bento, Christophe Trehin, Marie Monniaux, Jan Zethof, Michiel Vandenbussche

Plant Cell Advance Publication. Published on October 7, 2019, doi:10.1105/tpc.19.00162

RESEARCH ARTICLE

Divergent Functional Diversification Patterns in the SEP/AGL6/AP1 MADS-box Transcription Factor Superclade

Patrice Morel[1], Pierre Chambrier[1], Véronique Boltz[1], Sophy Chamot[1], Frédérique Rozier[1], Suzanne Rodrigues Bento[1], Christophe Trehin[1], Marie Monniaux[1], Jan Zethof[2] and Michiel Vandenbussche[1,*].

[1]Laboratoire Reproduction et Développement des Plantes, Univ Lyon, ENS de Lyon, UCB Lyon 1, CNRS, INRA, F-69342, Lyon, France
[2]Plant Genetics, IWWR, Radboud University Nijmegen, 6525AJ Nijmegen, The Netherlands
*Corresponding Author: michiel.vandenbussche@ens-lyon.fr

Short title: Analysis of the Petunia SEP/AGL6/AP1 Superclade

One sentence summary: Functional analysis of the petunia MADS-box gene SEP/AGL6/AP1 superclade compared to Arabidopsis and other species suggests major differences in the functional diversification of its members during evolution.

Keywords: SEPALLATA; APETALA1; AP1/SQUA; AGL6; MADS-box; floral meristem identity; inflorescence meristem identity, plant evolution; ABC model; Petunia; Arabidopsis; inflorescence architecture

The author responsible for distribution of materials integral to the findings presented in this article in accordance with the policy described in the Instructions for Authors (www.plantcell.org) is: Michiel Vandenbussche (michiel.vandenbussche@ens-lyon.fr).

ABSTRACT

Members of *SEPALLATA* (*SEP*) and *APETALA1* (*AP1*)/*SQUAMOSA* (*SQUA*) MADS-box transcription factor subfamilies play key roles in floral organ identity determination and floral meristem determinacy in the Rosid species Arabidopsis. Here, we present a functional characterization of the seven *SEP*/*AGL6* and four *AP1*/*SQUA* genes in the distant Asterid species *Petunia x hybrida* petunia. Based on the analysis of single and higher order mutants, we report that the petunia *SEP1*/*SEP2*/*SEP3* orthologs together with *AGL6* encode classical *SEP* floral organ identity and floral termination functions, with a master role for the petunia *SEP3* ortholog *FLORAL BINDING PROTEIN 2* (*FBP2*). By contrast, the *FBP9* subclade members *FBP9* and *FBP23*, for which no clear ortholog is present in Arabidopsis, play a major role in determining floral meristem identity together with *FBP4*, while contributing only moderately to floral organ identity. In turn, the four members of the petunia *AP1*/*SQUA* subfamily redundantly are required for inflorescence meristem identity, and act as B-function repressors in the first floral whorl, together with *BEN*/*ROB* genes. Overall, these data together with studies in other species suggest major differences in the functional diversification of the *SEP*/*AGL6* and *AP1*/*SQUA* MADS-box subfamilies during angiosperm evolution.

INTRODUCTION

Over the last two decades, the ABC model of floral organ identity has served as a genetic framework for the understanding of flower development in other species, and across evolution (Bowman et al., 2012). Members of the MADS-box transcription factor family play a central role in this model, and especially the MADS-BOX proteins encoding the floral B- and C-functions have been studied in a wide range of species (Krizek and Fletcher, 2005), providing a better understanding of the evolution and diversification of floral development at the molecular level. By contrast, much less comparative data is available for members of the *AP1*/*SQUA* and the *SEPALLATA* MADS-box transcription factor subfamilies. Compared to the B- and C-class MADS-box subfamilies, the *SEP* and *AP1*/*SQUA* subfamilies have substantially expanded via several gene duplication events during angiosperm evolution (Litt and Irish, 2003; Zahn et al., 2005). Together with reported extensive redundancy among individual *SEP* and among *AP1*/*SQUA* genes (see below), this makes comparative functional studies challenging, and probably underlies the relative lack of functional data in a broad range of species. Moreover, the extensive sequence similarity observed among members within both subfamilies may render the interpretation of phenotypes obtained by gene-silencing approaches (such as RNAi/co-suppression/VIGS) difficult. In addition, in several species members of the closely related *AGL6* MADS-box subfamily also perform SEP-like functions (Ohmori et al., 2009; Rijpkema et al., 2009; Thompson et al., 2009; Dreni and Zhang, 2016), adding further genetic complexity to a comparative analysis of the SEP function across species borders.

The *SEP* and *AP1*/*SQUA* MADS-box transcription factor families are unique to angiosperms, while *AGL6* genes are present both in gymnosperms and angiosperms (Becker and Theissen, 2003; Litt and Irish, 2003; Zahn et al., 2005). Interestingly, the *AGL6*, *SEP* and *AP1*/*SQUA* subfamilies together compose a monophyletic superclade within the MADS-box family (further referred to as the *AP1*/*SEP*/*AGL6* superclade), suggesting a common ancestral origin predating the angiosperm/gymnosperm divergence, although the evolutionary relationship between the different subfamilies had not been completely resolved (Purugganan et al., 1995; Purugganan, 1997; Becker and Theissen, 2003). A more recent phylogenetic analysis based on exon/intron structural changes suggests that *AGL6* genes are sister to both *SEP* and *AP1* subfamilies (Yu et al., 2016).

Thus far, Arabidopsis is the only core eudicot species for which a functional characterization of all its *AP1*/*SEP*/*AGL6* superclade genes has been achieved in sufficient detail, including the identification of redundant functions through higher order mutant analysis, but a wealth of functional data has been accumulated also in tomato and rice in recent years

(see further). The Arabidopsis *SEP* subfamily consists of four members, named *SEP1*, *SEP2*, *SEP3* and *SEP4*, and petals, stamens and carpels in the *sep1 sep2 sep3* triple mutant are transformed into sepals (Pelaz et al., 2000), while all floral organs in a *sep1 sep2 sep3 sep4* mutant develop as leaf-like organs (Ditta et al., 2004). This led to the conclusion that *SEP* genes are required for the identity of all floral organs, and function in a largely, but not completely redundant fashion. In addition, *SEP* genes were shown to be involved in floral meristem identity and determinacy (Pelaz et al., 2000; Ditta et al., 2004). SEP proteins are proposed to act as 'bridge proteins' enabling higher order complex formation (floral quartets) with the products of the homeotic B and C function organ identity genes, and to provide transcriptional activation capacity to these complexes (Honma and Goto, 2001; Theissen and Saedler, 2001; Immink et al., 2009; Melzer et al., 2009). These findings have inspired the addition of the SEP (or E-) function to the classic ABC model of floral development (Bowman et al., 1991; Coen and Meyerowitz, 1991), summarized in a floral quartet model (Theissen and Saedler, 2001). In contrast to the function of *AGL6* genes in other species, the two Arabidopsis *AGL6* subfamily members *AGL6* and *AGL13* do not seem to perform a SEP-like function in floral organ identity determination (Koo et al., 2010; Huang et al., 2012; Hsu et al., 2014). The Arabidopsis *AP1*/*SQUA* subfamily is composed of 4 members, of which the roles of *AP1*, *CAL* (*CAULIFLOWER*) and *FUL* (*FRUITFULL*) in floral development have been particularly well studied. Arabidopsis *ap1* mutants lack petals and have sepals displaying bract like features (Irish and Sussex, 1990; Mandel et al., 1992). For these reasons, *AP1* has been classified as an A-function gene in the ABC model, required for the identity specification of sepals and petals. Furthermore, *AP1* plays also a major role in specifying floral meristem identity, in a largely redundant fashion with *CAL* (Bowman et al., 1993; Kempin et al., 1995). *FUL* was initially identified for its unique role in Arabidopsis carpel and fruit development (Gu et al., 1998), but in addition was later shown to function redundantly with *AP1* and *CAL* to control inflorescence architecture (Ferrandiz et al., 2000).

To provide more insight in floral development and in the evolution of the floral gene regulatory network in higher eudicot species in general, we have been systematically analyzing the genetics underlying floral development in the Asterid species *Petunia x hybrida*. While the genes encoding the floral A, B and C- functions in petunia have been well characterized (Angenent et al., 1993; van der Krol et al., 1993; Kater et al., 1998; Kapoor et al., 2002; Vandenbussche et al., 2004; Rijpkema et al., 2006; Cartolano et al., 2007; Heijmans et al., 2012; Morel et al., 2017; Morel et al., 2018), only a few of the 10 previously described genes belonging to the large petunia *AP1*/*SEP*/*AGL6* superclade (Immink et al., 1999; Ferrario et al.,

2003; Immink et al., 2003; Vandenbussche et al., 2003a; Vandenbussche et al., 2003b; Rijpkema et al., 2009) have been functionally analyzed thus far.

Research on petunia *SEPALLATA* genes dates back a long time and provided, together with a study in tomato, the first indication of the existence of SEP-function in floral development: transgenic lines in which the *SEP3*-like petunia *FBP2* or tomato *TM5* genes were silenced by co-suppression both exhibited simultaneous homeotic conversion of whorls 2, 3, and 4 into sepal-like organs and loss of determinacy in the center of the flower (Angenent et al., 1994; Pnueli et al., 1994), a phenotype similar to that later found in Arabidopsis *sep1 sep2 sep3* mutants. However, at that time, multimeric complex formation of MADS-box proteins still remained to be discovered (Egea-Cortines et al., 1999), and it was not clear how many genes where co-suppressed in these lines. Therefore, the molecular basis of these phenotypes in petunia and tomato was not immediately understood. Later, it was shown in yeast that petunia SEP proteins also bind to B-class heterodimers and to C-class proteins, mediate quaternary complex formation with B- and C-class proteins and display transcriptional activation capacity (Ferrario et al., 2003), compatible with the proposed quartet model in Arabidopsis. Interestingly, among the six petunia SEP-like proteins, also clear differences in protein–protein interactions were revealed in a yeast 2-hybrid assay, suggesting functional diversification (Ferrario et al., 2003; Immink et al., 2003). Especially FBP2 and FBP5 showed a much broader range of interaction partners compared to the other petunia SEP proteins. Furthermore, it was shown *in planta* that petunia SEP proteins may be crucial to import at least some other MADS-box transcription factors into the nucleus (Immink et al., 2002).

Using a gene-specific approach, we showed that the *fbp2* co-suppression phenotype was indeed not gene specific, since single *fbp2* mutants showed only a very incomplete *sep-like* phenotype, with primarily the margins of the petals exhibiting a petal-to sepal homeotic conversion (Vandenbussche et al., 2003b). We also reported *fbp5* mutants that as single mutants develop as wild type. Flowers of *fbp2 fbp5* mutants, however, showed an enhanced phenotype compared to *fbp2* mutants: the sepaloid regions at the petal edges extended slightly further towards the center; sepal-like structures appeared on top of the anthers, and a sudden dramatic phenotype appeared in the ovary, which continued to grow long after development has arrested in wild-type (WT) flowers of comparable stages, resulting in a giant ovary. While the general architecture of the ovary was maintained (carpels containing an interior placenta), inside all ovules were homeotically converted to sepal-like organs (Vandenbussche et al., 2003b). This directly demonstrated that not only the identity of petals, stamens and carpels depends on SEP activity in petunia, but also ovule identity, as was also reported in Arabidopsis in the same

journal issue (Favaro et al., 2003). More recently, we demonstrated that petunia *AGL6* also exhibits SEP-like functions (Rijpkema et al., 2009), and performs a major role in petal identity, redundantly with *FBP2*. In addition, a function in stamen development was revealed by *fbp2 fbp5 agl6* triple mutant analysis. In line with the proposed SEP-function for AGL6, we found that AGL6 and FBP2 in yeast overall interact with the same the partners (Rijpkema et al., 2009).

Thus far, three petunia *AP1*/*SQUA* genes have been described, called *PFG*, *FBP26* and *FBP29* (Immink et al., 2003), and only the function of *PFG* was analyzed, using a co-suppression approach, resulting in a dramatic nonflowering phenotype, although the occasional development of single solitary flowers in these lines was also reported (Immink et al., 1999). However, as for the *FBP2* co-suppression line, the full-length coding sequence including the highly conserved MADS-domain was used to generate the co-suppression construct, questioning the specificity of the obtained phenotype.

To provide more insight in the functions of the *AP1*/*SEP*/*AGL6* superclade members in petunia, and more broadly in the evolutionary trajectory of the *AP1*/*SEP*/*AGL6* superclade in the core eudicots, we aimed to uncover unique and redundant functions of the complete *SEP*/*AGL6* and *AP1*/*SQUA* subfamilies during petunia flower development.

First, we present a genetic fine-dissection of the petunia SEP-function obtained from the analysis of a series of single and multiple knock-out mutants, combining putative null mutations in the six petunia *SEP* genes and *AGL6*. Most remarkably, we found that the *FBP9* subclade members *FBP9* and *FBP23*, for which no clear ortholog is present in Arabidopsis (Zahn et al., 2005), play an essential role in determining floral meristem identity together with *FBP4*, with only moderate contributions to the classic SEP floral organ identity function. Furthermore, we show that the petunia genetic equivalent of the Arabidopsis *sep1 sep2 sep3* mutant still displays residual B- and C-function activity, while a full *sepallata* phenotype was obtained in a sextuple *fbp2 fbp4 fbp5 fbp9 pm12 agl6* mutant. The analysis further suggests that the petunia *SEP3* ortholog *FBP2* performs a master floral organ identity SEP-function as in Arabidopsis. In addition, we have analyzed the dependence of homeotic gene expression on the SEP function, by comparing the dynamics of expression between wild-type and the sextuple *fbp2 fbp4 fbp5 fbp9 pm12 agl6* mutant.

Finally, we show that the petunia *AP1*/*SQUA* subfamily is composed of four members (*PFG*, *FBP26*, *FBP26* and the here described *euAP1* gene) that function in a largely redundant way. We found that they are required for inflorescence meristem identity, but surprisingly, *pfg fbp26 fbp29 euap1* mutants developed fully functional terminal flowers. In addition, we show that they act as B-function repressors in the first floral whorl, together with *BEN*/*ROB* genes

(Morel et al., 2017). Overall, comparison of these data with previous studies in mainly Arabidopsis, tomato and rice reveal major differences in the functional diversification of the *SEP*/*AGL6* and *AP1*/*SQUA* MADS-box subfamilies during evolution of the angiosperms.

RESULTS

Petunia Floral Development

To facilitate the comparison of the phenotypes presented in this study with the equivalent Arabidopsis mutants, we summarize first the relevant differences in WT floral architecture between petunia and Arabidopsis (Figure 1). Petunia flowers consist, from the outside towards the center, of five sepals partly fused at their basis, five large congenitally fused petals, five stamens of which the filaments are partly fused with the petal tube, and a central pistil composed of two congenitally fused carpels (Figure 1A). Some important differences in flower development between petunia and Arabidopsis, and relevant for this study, concern sepal identity, placentation topology and inflorescence architecture. Indeed in Arabidopsis, epidermal cell types and trichome architecture found on sepals can clearly be distinguished from those of leaves (Ditta et al., 2004). By contrast, petunia sepals display a similar kind of epidermal cell types as found in bracts and leaves, and are covered with the same type of multicellular trichomes (Figure 1C). While Arabidopsis sepals dehisce rapidly after fertilization of the flower and subsequently fall off together with petals and stamens, petunia sepals physiologically behave more as leaf-like organs: they stay firmly attached to the pedicel and may remain green, even long after the fruit has fully matured (Figure 1B). Note that the same occurs in flowers that were not fertilized (see further Figure 4F). The parietal placenta and ovules in Arabidopsis develop from the inner ovary wall, after termination of the floral meristem. In petunia, the central placenta arises directly from the center of the floral meristem in between the two emerging carpel primordia (Figure 1D), suggesting that the floral meristem is terminated later compared to Arabidopsis (Colombo et al., 2008). Finally, Petunia species develop a cymose inflorescence (Figure 1E, inset) as opposed to the raceme in Arabidopsis (reviewed in (Castel et al., 2010)). During petunia cymose inflorescence development, the apical meristem terminates by forming a flower, while an inflorescence meristem (IM) emerges laterally, repeating the same pattern (Souer et al., 1998). This results in the typical zigzag-shaped petunia inflorescence with alternating flowers on each node subtended by bracts.

Petunia *SEP*/*AGL6* Expression Analysis and Mutant Identification

Six *SEP* genes and one *AGL6* gene (Ferrario et al., 2003; Vandenbussche et al., 2003b; Rijpkema et al., 2009) were described in petunia compared to 4 *SEP* genes and 2 *AGL6*-like genes in Arabidopsis. A survey of the recently released *Petunia axillaris* and *Petunia inflata* genome sequences (Bombarely et al., 2016) indicated that these sequences represent the total number of *SEP*/*AGL6* genes in petunia (Supplemental Table 1). Several detailed and robust phylogenetic studies of the *SEP* family (Zahn et al., 2005; Yu et al., 2016) as well as the more limited phylogenetic analysis presented here (Figure 1F), identified *FBP2* as the sole *SEP3* ortholog in petunia, meaning that the petunia *SEP3* clade contains only one member as in Arabidopsis. Petunia *FBP5* and *PMADS12* (*PM12*) were shown to be the closest relatives of *SEP1* and *SEP2*, with the *FBP5*/*PM12* and *SEP1*/*SEP2* paralogous pairs originating from independent gene duplications in the lineages leading to petunia and Arabidopsis respectively. Finally, petunia *FBP4* grouped in the *SEP4* subclade, while *FBP9* and *FBP23* genes were members of the *FBP9* subclade, a subclass of *SEP* genes that is absent from the Arabidopsis genome and potentially may have been lost in the lineage leading to Arabidopsis (Malcomber and Kellogg, 2005; Zahn et al., 2005). The larger number of *SEP* genes in petunia compared to Arabidopsis is therefore entirely due to the presence of the two petunia *FBP9* subclade genes.

As expected based on their close taxonomic relationship, the petunia proteins overall showed the closest relationship with SEP/AGL6 members from tomato (The Tomato Genome Consortium, 2012; Soyk et al., 2017) compared to Arabidopsis and rice (Figure 1F). Like petunia, tomato contained one *AGL6* gene, one *SEP3* copy and two *FBP9* members, but slight differences in the number of genes belonging to the *SEP1*/*SEP2* and *SEP4* subclades could be observed between the two species. Notably, tomato contained only one *SEP1*/*SEP2* copy, while having two *SEP4*-like genes. Among the members of the tomato SEP/AGL6 family, the *SEP4-like RIN* gene initially received most of the attention, because the classical *rin* mutation has been widely used in tomato breeding as it improves shelf-life of tomato fruits when present in a heterozygous state, while the homozygous *rin* mutation prevents initiation of ripening (Vrebalov et al., 2002). Interestingly, more recent studies in tomato have shed a first light on the function of the enigmatic *FBP9* subclade genes. First of all, it was found that *SLMBP21*/*J2* (*JOINTLESS 2*) is required for the development of the pedicel abscission zone (Liu et al., 2014; Roldan et al., 2017; Soyk et al., 2017). Furthermore, a breakthrough functional study (Soyk et al., 2017) based on both natural and CRISPR induced mutant alleles showed that the two tomato *FBP9* clade genes *SLMBP21*/*J2* and *SlMADS1*/*EJ2* (*ENHANCER OF JOINTLESS 2*) have overlapping functions in meristem maturation and the control of inflorescence branching together with *LIN* (*LONG INFLORESCENCE*), the second tomato *SEP4-like* gene.

Remarkably, triple *j2 ej2 lin* knockout mutants exhibit a dramatic phenotype consisting of massively overproliferated sympodial inflorescence meristems (SIMs) without the formation of flowers, indicating that the transition towards FM identity is not made.

As a first step in the characterization of the complete *SEP*/*AGL6* clade in petunia, we performed RT-qPCR expression analysis (Figure 1G) in three floral bud developmental stages (Figure 1E) with the stage 1 floral bud sample also including very early flower primordia, bracts and the inflorescence meristem, and in various other tissues. This allows for a more quantitative analysis than a previous study by RNA gel blot and *in situ* hybridization (Ferrario et al., 2003). We detected important differences in expression levels among the *SEP*/*AGL6* genes and clear differences in expression patterns, both correlated with their phylogenetic position, suggesting functional divergence: *FBP2*, *FBP5*, and *AGL6* were the most abundantly expressed genes, reaching expression levels roughly tenfold higher than the *SEP4* homolog *FBP4*, and the *FBP9* subclade members *FBP9* and *FBP23*. Furthermore, *FBP2*, *FBP5* and *AGL6* expression was restricted to floral tissues, with expression levels strongly increasing during floral bud development, while *FBP4*, *FBP9* and *FBP23* were more broadly expressed, and expression levels did not show a strong upregulation during later stages of floral bud development. Expression outside the floral domain was most marked in bracts for *FBP4*, and in the inflorescence stem tissue for both *FBP4* and *FBP9*. One exception to these general differences observed between *SEP1*/*SEP2*/*SEP3*/*AGL6* and *SEP4*/*FBP9* genes was *PM12*, which was expressed ~100 fold lower than its close paralog *FBP5*, and for which expression was detected also in bracts and stems. For all genes analyzed, expression levels varied considerably between the different floral organs: Expression may be much lower in one particular organ type compared to the three other floral organs (e.g. very low *FBP2* and *FBP5* expression in sepals; low levels of *PMADS12*, *AGL6* and *FBP23* expression in stamens), or may peak in one specific floral organ (*FBP4* in sepals; *FBP9* in petals). Our results are in agreement with the *in situ* data previously obtained for *FBP2* and *FBP5*, showing mainly expression in the three inner floral whorls during early flower development, while some minor differences with the *PMADS12 in situ* data suggest that the *PM12* expression pattern is not constant as floral buds further develop (Ferrario et al., 2003).

To perform a functional analysis, we used a reverse genetics strategy (Koes et al., 1995; Vandenbussche et al., 2003b; Vandenbussche et al., 2008) to identify *dTph1* transposon insertions in the coding sequences of the petunia *SEP* and *AGL6* genes. In total, we identified and confirmed 16 independent transposon insertions *in planta*, including some earlier reported alleles (Vandenbussche et al., 2003b; Rijpkema et al., 2009) in all of the 7 different members

of the *SEP*/*AGL6* clade (Figure 1H). Because the 284 bp *dTph1* sequence encodes stop codons in all six possible reading frames, and based on their insert position (either disrupting the first exon encoding the MADS DNA binding domain, or the K-region required for protein-protein interactions in the case of the *fbp2* insertions, all of the selected insertion alleles most likely represent null alleles. We obtained and analyzed homozygous mutants for all insertion alleles, but remarkably, only homozygous mutants for *fbp2* insertions displayed floral homeotic defects (Figure 1H), suggesting extensive functional redundancy among the petunia *SEP*/*AGL6* genes, and that *FBP2* function is more essential than that of any other *SEP*/*AGL6* gene. These results clearly indicated the need for multiple mutant analyses to further uncover putative redundant functions.

The Petunia *fbp2 fbp5 pmads12* Mutant, Genetic Equivalent of the Arabidopsis *sep1 sep2 sep3* Mutant, Displays Floral Characteristics Indicating Residual B- and C-Function Activity

In Arabidopsis, the simultaneous loss of *SEP1*, *SEP2* and *SEP3* results in flowers consisting only of sepals (Pelaz et al., 2000). To compare the petunia genetic equivalent, we aimed to analyze *fbp2 fbp5 pm12* triple mutants (Figure 2). As mentioned earlier, of the three single mutants, only *fbp2* mutants displayed a phenotype different from WT (Figures 2A to 2D). Moreover, *fbp2*/+ *fbp5 pm12* flowers (Figure 2E) developed morphologically as WT, demonstrating that *FBP2* even in a heterozygous state can fully compensate for the loss of *FBP5* and *PM12* functions. In addition, *fbp2 pm12* double mutants were not markedly different from *fbp2* single mutants (Figure 2F), in contrast to the earlier reported *fbp2 fbp5* mutants (Figures 2G to 2K) and (Vandenbussche et al., 2003b). However, *fbp2 fbp5 pm12* flowers could be easily distinguished from *fbp2 fbp5* flowers: a clear enhancement of stamen to sepal identity could be observed in the third whorl, although still some antheroid tissue remained, as in *fbp2 fbp5* mutants (Figure 2M). Furthermore, while the extremely enlarged *fbp2 fbp5* mutant pistil still exhibited partial carpel identity, the carpels of *fbp2 fbp5 pm12* mutants acquired clear sepal/leaf-like epidermal characteristics (Figures 2N to 2Q), and were densely covered with trichomes. The latter are never observed on WT pistils, and only at very low frequency on *fbp2 fbp5* pistils (Figure 2N). Furthermore, no stigma and style structures remained in the triple mutant, but the overall internal organization of the ovary was maintained, with a placenta structure covered by a few hundred leaf-like organs that represented homeotically converted ovules, as observed in *fbp2 fbp5* mutants (Figures 2K and 2L). In the second whorl of *fbp2 fbp5 pm12* flowers, the partial petal to sepal conversion at the corolla border was only subtly

enhanced compared to *fbp2 fbp5* mutants (Figures 2G and 2H). Given that the effect of the *pm12* mutation only became apparent in an *fbp2 fbp5* mutant background, we conclude that *PM12* plays a less essential role than its close paralog *FBP5*. Overall, the remnant petal and stamen tissues and the maintenance of a placenta structure in *fbp2 fbp5 pm12* flowers show that unlike in Arabidopsis, genes outside the *SEP3* and *SEP1*/*SEP2* subfamilies are able to rescue part of the B- and C-functions in a petunia *sep1 sep2 sep3* mutant background.

The *FBP9* Subclade Genes *FBP9* and *FBP23* Function as Floral Meristem Identity Genes together with *FBP4*

We showed earlier that petunia *AGL6* is one of the genes outside the classical SEP1/SEP2/SEP3 group that plays a prominent role in performing a SEP-like floral organ identity function, especially in the determination of petal identity, redundantly with *FBP2* (Rijpkema et al., 2009). However, *FBP4* as a *SEP4*-like gene may also participate, as found in Arabidopsis (Ditta et al., 2004) and potentially also *FBP9* and *FBP23*, the petunia representatives of the *FBP9* subclade.

Earlier we found that the *fbp9*, *fbp23* and *fbp4* single mutants displayed a WT phenotype (Figure 1H), and that expression levels of all three genes peak early during floral developmental stages compared to the other petunia *SEP* genes and *AGL6* (Figure 1G), potentially indicating a redundant (common) function for *FBP4*, *FBP9* and *FBP23*. Indeed, a functional overlap was recently demonstrated among corresponding SEP subclade members in tomato (Soyk et al., 2017).

To test such a putative functional redundancy among the petunia *FBP9*, *FBP23* and *FBP4* genes, we first created and analyzed *fbp9 fbp23* double mutants, since *FBP9* and *FBP23* are close paralogs belonging to the same *FBP9 SEP*-subclade. Interestingly, we found that *fbp9 fbp23* mutants were dramatically affected in their inflorescence architecture, with new inflorescence shoots developing instead of flowers, resulting in a highly branched inflorescence structure. However, flower development was not completely abolished in these mutants, because after several weeks of a highly branched inflorescence development, frequently a flower appeared on one or more branches of the same plant, after which these branches switched again to the initial phenotype (Figures 3B and 3F). This indicated that the capacity to form floral meristems was not completely abolished in *fbp9 fbp23* mutants and that (an)other factor(s) can partly rescue floral meristem determinacy in the absence of *FBP9*/*FBP23* function. Because we assumed *FBP4* being a likely candidate, we next analyzed *fbp4 fbp9 fbp23* triple mutants. Indeed, we found that the *fbp9 fbp23* phenotype was further enhanced in these triple mutants, resulting in a highly branched flowerless inflorescence architecture (Figures 3C, 3G

and 3H), phenotypically very similar to that reported earlier for the petunia floral meristem identity mutant *alf* (Souer et al., 1998), with *ALF* being orthologous to Arabidopsis *LEAFY* (*LFY*) (Weigel et al., 1992) and snapdragon *FLORICAULA* (*FLO*) (Coen et al., 1990) genes. Note that over a long period (> 6 months) of highly branched inflorescence development, some triple mutants produced 1-2 isolated flowers, while other individuals never flowered at all.

To study the *fbp4 fbp9 fbp23* phenotype in more detail, we analyzed *fbp4 fbp9 fbp23* inflorescence apices by scanning electron microscopy in comparison with WT (Figures 3I to 3L). At very early developmental stages, the *fbp4 fbp9 fbp23* plants exhibited a phenotype very comparable to *alf* mutants (Souer et al., 1998): as in *alf* mutants, the bifurcation pattern of *fbp4 fbp9 fbp23* inflorescence apices was similar to WT, but the two resulting meristems both behaved as inflorescence meristems, as indicated by the continuous bifurcation of each newly formed meristem and the repetitive formation of bracts flanking these meristems. Together, this indicates that floral meristems in *fbp4 fbp9 fbp23* mutants are homeotically transformed into inflorescence meristems.

Finally, floral meristem identity was not visibly affected in *fbp4 fbp9 fbp23*/+ and *fbp4 fbp23 fbp9*/+ plants, as judged by the presence of a normal cymose inflorescence architecture in these mutant combinations (Figures 3M to O). This shows that the presence of either *FBP9* or *FBP23* in heterozygote state is sufficient to rescue floral meristem identity. Together with the already strong phenotype observed in *fbp9 fbp23* plants compared to *fbp4 fbp9 fbp23* plants (Figures 3B to 3C, 3F to 3G, 3P to 3Q), we conclude that the *FBP9* clade members *FBP23* and *FBP9* play a major role in floral meristem identity determination in a largely redundant fashion, while *FBP4* is involved in the same function, but plays a less essential role compared to the *FBP9*/*FBP23* gene pair.

Although the phenotypes of tomato *j2 ej2 lin* and petunia *fbp9 fbp23 fbp4* mutants at first sight do not look very similar (see discussion), overall, this shows that in both species, *FBP9* clade genes together with a *SEP4* gene play an essential role in floral meristem identity, different from the classical SEP organ identity functions.

To test whether *FBP4*, *FBP9* and *FBP23* also function later in conferring floral organ identity, we introduced the corresponding mutations into the *fbp2* mutant background, the only petunia *sep* mutation with a visible phenotype as a single mutant. However, we found that flowers of *fbp2 fbp4*, *fbp2 fbp9* and *fbp2 fbp23* mutants were not markedly different from *fbp2* mutants (Figures 3R to 3U), while *fbp2 fbp4 fbp23* and *fbp2 fbp4 fbp9* flowers only showed a moderate enhancement of the *fbp2* petal-to-sepal conversion phenotype (Figure Figures 3V to 3W). In *fbp2 fbp4 fbp23* flowers, the green margin appeared to be broader in all five petals

while in *fbp2 fbp4 fbp9* flowers this was most visible in the two basal petals. In comparison with the earlier described floral phenotypes of *fbp2 fbp5* (Vandenbussche et al., 2003b), *fbp2 agl6*, *fbp2 fbp5 agl6* (Rijpkema et al., 2009) and *fbp2 fbp5 pmads12* mutants, this suggests that *FBP4*, *FBP9* and *FBP23* do play a role in floral organ identity, but contribute only moderately to this function compared to the petunia *SEP1*/*SEP2*/*SEP3* homologs and *AGL6*. Note that we also obtained *fbp2 fbp4 fbp9 fbp23* quadruple mutants, but as expected, these developed a highly branched flowerless inflorescence structure as in *fbp4 fbp9 fbp23* mutants.

The Sextuple *fbp2 fbp4 fbp5 fbp9 pm12 agl6* Mutant Displays a Classic *sepallata* Phenotype

By analyzing *AGL6*, *FBP2* and *FBP5* functions and the *fbp2 fbp5 pmads12* and *fbp4 fbp9 fbp23* triple and *fbp2 fbp4 fbp9 fbp23* mutants, we could reveal specific/specialized SEP functions for certain members of the petunia *SEP*/*AGL6* clade and surprisingly, the requirement of *FBP9*/*FBP23* function (and to a lesser extend *FBP4*) for floral meristem identity, as was also recently shown in tomato. However, a classic floral *sepallata* phenotype as described for Arabidopsis was not obtained, indicating further redundancy, possibly shared between the majority of the petunia *SEP*/*AGL6* genes. To test this further, we embarked on a long-term crossing scheme aimed to combine all of the *sep*/*agl6* mutant alleles in a single plant. However, we chose to exclude the *fbp23* mutation in this scheme since this would completely abolish flower formation when combined with the *fbp9* and *fbp4* mutations and thus prevent visualization of additive floral phenotypes. After years of crossing, we finally obtained homozygous sextuple *fbp2-332 fbp4-44 fbp5-129 fbp9-90 pm12-37 agl6-118* mutant plants, hereafter referred to as sextuple *sep*/*agl6* mutants. In contrast to the earlier described lower order mutants, all organs in the flowers of sextuple *sep*/*agl6* mutants were green and densely covered by trichomes (Figure 4), exhibiting sepal/leaf-like characteristics (Figures 4A to 4E). Note that as mentioned earlier, it is not possible to discriminate between sepal, bract and leaf identity in petunia based on epidermal cell characteristics (Figure 1C). As expected, scanning electron microscopy of these organs revealed the conversion of the typical petal, stamen and carpel epidermal cell types into epidermal cells characteristic for sepals, bracts and leaves, including stomata and multicellular trichomes (Figure 4E). The second whorl, which in WT consists of five large brightly colored fused petals, was occupied by five green organs that remained fused at their bases (Figure 1C). Although dramatically smaller than WT petals, they remained larger than first whorl sepals. Similarly, in the third whorl, the five stamens were replaced by sepal/leaf like organs. The overall shape of these organs did retain some of the stamen architecture, since the region corresponding to the WT stamen filament remained

smaller compared to the more leaf blade-like upperparts. Stamen filaments in WT are fused along half of their length with the inside of the petal tube. By contrast, third whorl organs in the sextuple mutant completely lost this partial fusion. In the fourth whorl, normally occupied by two carpels that are entirely fused and enclose the placenta and ovules, two (sometimes three) unfused sepal/leaf-like organs were found. Internally, the placenta was entirely replaced by a new emerging flower reiterating the same floral phenotype (Figure 1D). Thus in contrast to lower order *sep* mutants, the sextuple mutant was fully indeterminate. In the majority of the flowers (Figure 4F), this secondary flower further developed and emerged from the primary flower supported by a pedicel, while containing on itself another flower in its center. This third flower usually did not further grow out, although occasionally we observed up to three consecutive fully developed flowers (Figure 4F). Note that the sextuple *sep*/*agl6* mutant displayed a normal cymose inflorescence architecture as in WT (Figure 4F), in sharp contrast to *fbp4 fbp9 fbp23* mutants. This demonstrates that *FBP23* alone can fully rescue floral meristem identity in a sextuple mutant background, but not floral organ identity.

Homeotic Gene Expression in Sextuple *sep*/*agl6* Mutant Flowers

To further characterize the sextuple *sep*/*agl6* mutant at the molecular level, we quantified and compared the dynamics of homeotic gene expression levels between WT and the sextuple mutant (Figure 4G) at three different stages of floral bud development, as described earlier (Figure 1E). Encoding of the B-function in petunia is more complex compared to Arabidopsis and Antirrhinum, and involves the two PI/GLO-like MADS-box transcription factors *Petunia hybrida GLO1* and *GLO2*, the DEF/AP3 ortholog *PhDEF*, and *PhTM6*, the petunia representative of the ancestral B-class TM6 lineage that has been lost in Arabidopsis, but which is present in many species (Angenent et al., 1993; van der Krol et al., 1993; Vandenbussche et al., 2004; Rijpkema et al., 2006). In WT, we found that all four B-class genes were progressively upregulated as floral buds developed, with an upregulation from stage 1 to stage 3 varying roughly from three to six times, depending on the gene. In the sextuple mutant, we observed expression levels of *PhGLO1*, *PhGLO2* and *PhDEF* initially similar to WT in the youngest stage analyzed. However, upregulation in older stages was strongly affected, especially for *PhGLO1* and *PhGLO2*, which remained expressed at initial levels. *PhDEF* remained progressively upregulated in the different sextuple mutant samples, but reached only one third of the expression compared to WT in the final stage. By contrast, *PhTM6* expression levels were strongly downregulated from stage 1 floral buds onwards, remaining at similarly low levels in the two older stages.

The C-function in petunia is redundantly encoded by *PMADS3* and *FBP6*, orthologs of Arabidopsis AG and SHP1/2 respectively (Heijmans et al., 2012; Morel et al., 2018). As for the B-function genes, *FBP6* and *PMADS3* expression in WT is progressively upregulated in developing floral buds (6,5 and 11 times respectively), and initial expression levels in stage 1 buds were very similar between WT and sextuple mutants for both C-class genes. Both C-genes still displayed a clear upregulation in the older sextuple mutant flower buds, and seemed in general less affected by the sextuple loss of SEP/AGL6 function than the B-function genes, especially in stage 2. In stage 3 buds, *FBP6* expression was not different between WT and sextuple mutants, while *PMADS3* in the sextuple mutant was expressed at around 50% of its WT levels. *FBP11* is a petunia D-lineage MADS-box gene orthologous to *STK* (Angenent et al., 1995; Colombo et al., 1995), and that with *FBP7* (another D-lineage member) and the C-genes *PMADS3* and *FBP6* redundantly is required to confer ovule identity, and to arrest the floral meristem (Heijmans et al., 2012). Consistent with its later function in floral development, the *FBP11* expression profile showed a very strong upregulation in the WT developmental series (~30 fold). By contrast, in the sextuple mutant samples, *FBP11* expression was barely detectable in all stages tested.

Finally, we choose to monitor the expression of petunia *UNS* (*UNSHAVEN*), a member of the *SOC1* subfamily, because of its particular expression pattern reported to be mainly restricted to green tissues including stems, leaves, bracts and the first whorl (sepals) in the flower (Immink et al., 2003; Ferrario et al., 2004). Moreover, *UNS* ectopic expression was shown to confer leaf-like characteristics to floral organs. We first used the cDNA series from Figure 1F to analyze its expression pattern in a more quantitative manner compared to earlier gel blot data, confirming highest expression levels in bracts, inflorescence stems, and in the sepals within the flower (Supplemental Figure 1). In the WT developmental series, we found *UNS* to be progressively downregulated as flower buds further developed, corresponding to a ~4 fold drop in expression levels compared to the youngest stage (Fig 4G). Interestingly, *UNS* was expressed at higher levels in all sextuple mutant floral bud stages compared to WT, with the largest difference found in the oldest bud stage (~ 5-fold upregulation compared to WT). Moreover, a linear downregulation as in WT was not observed.

The Petunia *AP1*/*SQUA* Subfamily: Phylogeny, Expression Analysis and Mutant Identification

We found that the petunia *SEP* genes *FBP9*, *FBP23* and *FBP4* function primarily as floral meristem identity genes, a function which is in Arabidopsis mainly associated with

members of the *AP1*/*SQUA* MADS-box subfamily (Irish and Sussex, 1990; Mandel et al., 1992; Kempin et al., 1995; Ferrandiz et al., 2000). This raised the obvious question to what extent the petunia *AP1*/*SQUA* members are implicated in floral meristem identity determination. For these reasons, we aimed to functionally analyze the members of the petunia *AP1*/*SQUA* subfamily. Thus far, three petunia *AP1*/*SQUA* genes have been described, called *PFG*, *FBP26* and *FBP29* (Immink et al., 1999; Immink et al., 2003). In addition, based on sequence similarity, we identified a fourth *AP1*/*SQUA* member by the presence of an insertion mutant and associated transposon flanking sequence encountered in our transposon flanking sequence database, which we have called *Ph-euAP1* (*Petunia x hybrida euAP1*), based on the presence of the highly conserved euAP1 motif (Litt and Irish, 2003; Vandenbussche et al., 2003a) in its C-terminus, as also found in the Arabidopsis *AP1* and *CAL* genes (Supplemental Figure 2A). To provide further proof for the *euAP1* classification of the new Petunia AP1/SQUA member, we conducted a phylogenetic analysis (Figure 5) including all *AP1*/*SQUA* subfamily members from Arabidopsis, tomato (Hileman et al., 2006; The Tomato Genome Consortium, 2012 and rice (Lee et al., 2003; Yu et al., 2016). Similar to the SEP/AGL6 phylogenetic analysis, overall the petunia proteins showed the closest relationship with AP1/SQUA members from tomato (Figure 5A), while all four rice AP1 members grouped apart from the eudicot proteins as shown previously (Yu et al., 2016). The analysis further showed that petunia *euAP1* indeed is orthologous to the tomato *MACROCALYX* (*MC*) gene (Vrebalov et al., 2002) and the Arabidopsis *AP1* and *CAL* genes, all previously demonstrated as belonging to the *euAP1* clade (Litt and Irish, 2003; Yu et al., 2016). Petunia therefore is similar to tomato in having only one *euAP1* clade member compared to two members in Arabidopsis. *MC*, the tomato *euAP1* representative, was shown to regulate sepal size, fruit abscission and maintenance of inflorescence meristem identity. Indeed, *mc* mutants develop flowers with enlarged sepals, have an incomplete pedicel abscission zone, and develop inflorescences that revert to vegetative growth after forming two to three flowers (Vrebalov et al., 2002; Nakano et al., 2012; Yuste-Lisbona et al., 2016).

The previously described *FBP29* gene fell into the *AGL79* subclade to which the tomato genes *MBP10* and *MBP20* also belonged, while the *PFG and FBP26* genes grouped into the *euFUL* subclade together with the tomato *FUL1* (*TDR4*/*TM4*) and *FUL2* (*MBP7*) genes as previously shown (Yu et al., 2016). While stable mutants remain to be described for these four tomato genes, RNAi mediated downregulation of *FUL1* and *FUL2* indicate a role for these genes in fleshy fruit ripening (Bemer et al., 2012; Shima et al., 2013; Wang et al., 2014). Furthermore, a role for *MBP20* and *FUL1* was proposed in the regulation of compound leaf

development (Burko et al., 2013). Finally, to date no function has been proposed for tomato *MBP10* but an evolutionary study of the *FUL* genes in the Solanaceous family suggest that the *MBP10* lineage, which is absent in petunia, may be undergoing pseudogenization (Maheepala et al., 2019). A sequence analysis of the *Petunia axillaris* and *Petunia inflata* genome sequences (Bombarely et al., 2016) further indicated that *euAP1*, *PFG*, *FBP26* and *FBP29* represent the total number of *AP1*/*SQUA* family members in petunia (Supplemental Table 1), similar to the size of the *AP1*/*SQUA* subfamily in Arabidopsis and rice, and one less compared to tomato (due to the absence of a *MBP10* lineage member in petunia).

A quantitative expression analysis in different tissues and three floral bud developmental stages in WT (Figure 5B) showed that the expression patterns of the four genes were quite similar, although some minor differences did exist. Interestingly, expression levels of all four genes gradually decreased during floral bud development, suggesting an early developmental function, similar as what we observed for e.g. *FBP9* and *FBP4*. Furthermore, during later flower development, moderate expression levels were detected in sepals, petals (except for *FBP29*) and carpels, while expression in stamens was considerably lower compared to the other floral organs. The four genes were also well expressed in inflorescence stem tissues as well as in bracts (with the exception of *Ph-euAP1*). Finally, *PFG* showed the broadest expression pattern, since moderate expression levels were also observed in vegetative apices and leaves. In addition, the peak values of *PFG* expression levels were around tenfold higher compared to those of *Ph-euAP1*, *FBP26* and *FBP29*. The *PFG* expression data were in line with the broad expression pattern previously observed by RNA gel blot analysis and *in situ* hybridization (Immink et al., 1999), which revealed *PFG* expression in vegetative, inflorescence and floral meristems, in newly formed leaves, the vascular tissues, during early flower organ development and in carpel walls and ovules during later phases of pistil development.

To determine the function of the four petunia *AP1*/*SQUA* genes, we screened for *dTph1* transposon insertions in their coding sequences, similarly as for the *SEP* genes. In total, we identified and confirmed 6 independent transposon insertions *in planta* (Figure 5C), including two earlier reported alleles (Vandenbussche et al., 2003b), potentially yielding putative null mutants for all four genes based on the insertion position of the *dTph1* transposon, either disrupting the first exon encoding the MADS DNA binding domain or the K-region required for protein-protein interactions in the case of the *euap1* allele. We obtained and analyzed homozygous mutants for all insertion alleles, but all these homozygous mutants developed normally (Figure 5C). Moreover, when we analyzed some double mutants to overcome putative

genetic redundancy, flowers in these double mutants developed normally, and inflorescence architecture was not affected (Supplemental Figure 2B).

Petunia *AP1*/*SQUA* Family Members are Required for Inflorescence Meristem Identity

Because of the absence of clear phenotypes in the above-described mutants, we decided to create and analyze *pfg fbp26 fbp29 euap1* quadruple mutants (Figure 6). Remarkably, the flowers that developed on these quadruple mutants were fertile, and organ identity of the carpels, stamens and petals was not visibly affected (Figures 6A to 6C). However, sepals were considerably enlarged and contained sectors that exhibited homeotic conversion towards petal identity, as indicated by the red pigmentation and the presence of petal conical cells in these regions (Figure 6D). Overall, the general mildness of the *pfg fbp26 fbp29 euap1* flower phenotype was very surprising, compared to the already dramatic phenotypes found in Arabidopsis *ap1* single and *ap1 cal* double mutants, and compared to the complete absence of flowers in *ap1 cal ful* triple mutants (Irish and Sussex, 1990; Mandel et al., 1992; Kempin et al., 1995; Ferrandiz et al., 2000).

Quadruple *pfg fbp26 fbp29 euap1* mutants did display a severe phenotype in inflorescence development. In fact, the normal cyme inflorescence architecture was completely abolished, and instead a large number of leaves were produced from the main apical meristem before terminating into a solitary flower (Figures 6E and 6G). In addition, branches that developed from the base of the plant followed exactly the same developmental pattern (Figure 6L). The leaves produced on the main stem and side branches were generated in a spiral phyllotaxy (Figures 6F and 6Q), characteristic of vegetative development (Figure 6P), in contrast to the opposite positioning of bracts in a WT inflorescence meristem. Finally, after the production of usually >25 leaves, this vegetative meristem was fully converted into a floral meristem resulting in a solitary flower (Figures 6H to 6I) as opposed to the normal cyme inflorescence structure in WT (Figure 6M). Note that quadruple mutant flowers consistently displayed an increase in floral organ number (e.g. the flower shown in Figure 6A has 10 petals), possibly because the full conversion of the vegetative meristem into a floral meristem resulted in a larger floral meristem size. In addition, the corolla of these flowers was not always properly organized, as the petal tube was often disrupted on one side.

Once this terminal flower was fully developed, new branches started to grow from vegetative meristems that were present in the axils of the leaves further down on the stem (Figure 6I). These branches produced again a large number of leaves before terminating with a solitary flower (Figure 6X), after which the same process was repeated. Together these results

indicate that petunia *AP1*/*SQUA* genes are required to establish inflorescence meristem identity and associated cymose branching of the petunia inflorescence.

Interestingly, intermediate phenotypes could be observed in different triple mutants in which the fourth *AP1* subfamily member was still in a heterozygous state (Figures 6S to 6Q), resulting in inflorescences in which each time several leaves developed before the next flower-bearing node was produced. Together this indicates that all four genes contribute to cymose inflorescence development in petunia.

Petunia *AP1*/*SQUA* Family Members Repress the B-Function in the First Whorl in Concert with the *ROB*/*BEN* Genes.

The partial sepal-to-petal homeotic conversion in flowers of *pfg fbp26 fbp29 euap1* mutants (Figure 6D) suggests that petunia *AP1*/*SQUA* genes negatively regulate the B-function in the first floral whorl. Recently we demonstrated that the *AP2*-type *REPRESSOR OF B* (*ROB1*), *ROB2* and *ROB3* genes repress the B-function in the first whorl, together with *BEN*, a TOE-type *AP2* gene (Morel et al., 2017). To further explore the implication of the petunia *AP1*/*SQUA* genes in patterning the B-function, we tested their genetic interaction with *ROB* genes. We crossed *pfg fbp26 fbp29 euap1* and *rob1 rob2 rob3* mutants and screened progenies for an enhanced sepal-to-petal homeotic conversion phenotype compared to *pfg fbp26 fbp29 euap1* and *rob1 rob2 rob3* mutants. Among a large progeny, we found individuals displaying the *pfg fbp26 fbp29 euap1* inflorescence phenotype while bearing terminal flowers of which the first whorl organs showed a much more pronounced sepal-to-petal conversion compared to *pfg fbp26 fbp29 euap1* mutants. We genotyped several of these plants for the seven insertions, and found that plants with the strongest phenotype were *rob1 rob2*/+ *rob3 pfg fbp26 fbp29 euap1* (Figures 6J and 6K). Flowers of these mutants had first whorl organs that clearly formed the beginning of a petal tube (Figure 6J), although not fused along its entire length, and with strongly expanded petaloid regions compared to the first whorl organs of *pfg fbp26 fbp29 euap1* flowers (Figures 6D and 6K). The presence of pale pigmentation at the basal end of the organs and bright red at the distal end (Figure 6K) was also characteristic for the modular tube/corolla architecture of a WT petunia petal (Figures 1A and 2I). For comparison, first whorl sepals of *rob1 rob2*/+ *rob3* plants had a phenotype similar to WT (Figures 6N to 6O), while *rob1 rob2 rob3* flowers exhibit a very subtle sepal-to-petal conversion at the margins of their sepals, and which is only clearly visible in the first 2–3 flowers that develop (Morel et al., 2017). Although we did not obtain plants homozygous for all seven mutations, the synergistic interaction observed between *rob1 rob2*/+ *rob3* and *pfg fbp26 fbp29 euap1* mutations strongly supports a

role for petunia *AP1*/*SQUA* genes in repressing the B-function in the first whorl, together with the *ROB*/*BEN* genes.

DISCUSSION

A Comparison of *SEP*/*AGL6* and *AP1*/*SQUA* Functions in Petunia, Arabidopsis, Tomato and Rice

In this study, we exploited the natural *dTph1* transposon mutagenesis system in petunia to identify mutants for all 11 members of the petunia *AP1*/*SEP*/*AGL6* superclade, and created a series of higher order mutants to uncover putative redundant functions. Here we discuss and compare our findings with the available functional data from mainly Arabidopsis, tomato and rice (see Figures 1F and 5A for the composition of their SEP/AGL6 and AP1/SQUA subfamilies). Petunia and tomato on the one hand, and Arabidopsis on the other hand are representatives of the Asterids and Rosids respectively, which constitute the two major groups in the core eudicots, and are thought to have diverged >100 million years ago (Moore et al., 2010). Comparison of the molecular mechanisms controlling flower development in these species therefore helps to assess conservation and divergence of the floral regulatory gene network in the core eudicots (Vandenbussche et al., 2016). Petunia and tomato both belong to the Solanaceous family, and the lineages leading to petunia and tomato are estimated to have diverged around 30 MYA (Bombarely et al., 2016). Their close relationship is indeed reflected in a high degree of sequence similarity between tomato/petunia orthologous pairs in the AP1/SEP/AGL6 superclade (see also Supplemental Data Files 1, 2, 3 and 4), which makes the petunia/tomato comparison particularly well suited to evaluate functional diversification patterns on a shorter evolutionary time-scale, as opposed to the comparison with the distant monocot model species rice.

Implication of *SEP and AGL6* Gene Functions in Floral Organ Identity

Our genetic analysis in petunia indicates that its *SEP3* ortholog *FBP2* encodes the major *SEP* organ identity function: *FBP2* is capable of fully rescuing flower development in a *fbp2*/+ *fbp5 pm12* mutant background, and *fbp2* is the only *sep* single mutant with a clearly visible phenotype. In Arabidopsis, all available genetic data indicate that *SEP3* is also the most important *SEP* gene. Indeed, it was reported that single *sep3* mutants display a phenotype on their own, showing a mild petal to sepal conversion, while *sep1*, *sep2* and *sep4* single mutants showed no developmental abnormalities (Pelaz et al., 2001). Secondly, *sep1 sep2 sep4* mutants show no significant perturbation of floral organ development, indicating that *SEP3* can fully

rescue WT development in a triple mutant background (Ditta et al., 2004). Thus *SEP3* seems to perform a master SEP floral organ identity function in both species.

While the gene-silencing approaches used to analyze *SEP3* function in tomato and rice do not yet allow such detailed conclusions, these experiments suggest that their *SEP3* orthologs play also a major role in floral organ identity: Tomato *TM5* co-suppression lines genes exhibited homeotic conversion of whorls 2, 3, and 4 into sepal-like organs and loss of determinacy in the center of the flower (Pnueli et al., 1994) and a Y2H study found that TM5 was the preferred bridge protein of the 5 SEP tomato proteins tested (Leseberg et al., 2008). Transgenic lines carrying a construct aimed at simultaneously downregulating the two *SEP3-like* rice *OsMADS7* and *OsMADS8* genes were late flowering, and carried flowers exhibiting partial homeotic conversions of the floral organs in the three inner whorls into palea/lemma-like organs, and a partial loss of floral determinacy (Cui et al., 2010).

Arabidopsis *sep1 sep2 sep3* mutants display a full conversion of petals, stamens and carpels into sepals, and flowers are fully indeterminate (Pelaz et al., 2000). By contrast, the genetically equivalent *fbp2 fbp5 pmads12* mutant in petunia retains -albeit reduced- petal and stamen tissues, and the basic organization of the placenta structure in the flower center is maintained. Thus unlike in Arabidopsis, genes outside the *SEP3* and *SEP1*/*SEP2* clades are able to rescue part of the B- and C-functions in a petunia *sep1*/*sep2*/*sep3* mutant background. We identified petunia *AGL6* as one of these genes (Rijpkema et al., 2009). Similarly, the two rice *AGL6* genes *OsMADS6*/*MFO1* and *OsMADS17* perform *SEP-like* functions, partly in a redundant fashion with the *SEP* gene *OsMADS1*/*LHS1* (Ohmori et al., 2009; Dreni and Zhang, 2016). More recently, a floral organ identity function was also proposed for the tomato *AGL6* gene, based on RNAi (Yu et al., 2017). Despite that the Arabidopsis genome encodes two *AGL6* homologs (*AGL6* and *AGL13*), the phenotype of the *sep1 sep2 sep3* mutant demonstrates that Arabidopsis *AGL6* genes may have lost most of their SEP-like activity compared to petunia, rice and tomato *AGL6* genes, in agreement with the diverse proposed functions for Arabidopsis *AGL6* and *AGL13* (Koo et al., 2010; Huang et al., 2012; Hsu et al., 2014).

Furthermore, we showed that in a petunia sextuple *sep*/*agl6* mutant a full *sepallata* phenotype was obtained, including complete loss of floral meristem termination. Remarkably, the obtained phenotype was similar to that of the earlier described *FBP2* co-suppression line (Ferrario et al., 2003), demonstrating the efficiency of co-suppression to silence multiple genes simultaneously. The expression levels of all six petunia *SEP* genes (but not of *AGL6*) were monitored in the co-suppression line, but only *FBP2* and *FBP5* were found to be

downregulated. This strongly suggests that other genes were silenced at the post-transcriptional level as was reported to frequently occur in gene silencing experiments (Stam et al., 1997). Measuring mRNA levels of paralogous genes thus appears to be a limited method to assess the specificity of a silencing construct.

The addition of the *sep4* mutation to the Arabidopsis triple *sep1 sep2 sep3* mutant resulted in the conversion of sepal-like organs into leaf-like organs, indicating that *SEP* genes are required to specify sepal identity (Ditta et al., 2004). The fact that we could not observe a transition from sepal towards leaf-identity in the sextuple *sep*/*agl6* mutant is most likely directly related to the 'leaf'-like identity of petunia WT sepals. Such basic differences in sepal identity between Arabidopsis and other species such as petunia may be contributing to the difficulties to formulate a broadly applicable A-function (Litt, 2007; Causier et al., 2009).

Transgenic lines in which at least four of the rice *SEP-like* genes (*OsMADS1*/*LHS1* (*LEAFY HULL STERILE1*)), *OsMADS5*, *OsMADS7* and *OsMADS8*) were downregulated, showed homeotic transformation of all floral organs except for the lemma into leaf-like organs (Cui et al., 2010), reminiscent of the Arabidopsis *sep1 sep2 sep3 sep4* quadruple mutant flower phenotype. Remarkably however, severe loss-of-function mutations in the *LOFSEP* gene *OsMADS1*/*LHS1* alone can cause complete homeotic conversion of organs of the three inner whorls into lemma/palea-like structures, and loss of floral meristem determinacy (Agrawal et al., 2005), while also dominant-negative and milder phenotypes were reported for other *OsMADS1*/*LHS1* alleles (Jeon et al., 2000; Chen et al., 2006). More recently, Wu and colleagues specifically investigated unique and redundant functions of the three *LOFSEP* genes using mutant alleles and found that *OsMADS1*/*LHS*, *OsMADS5*, and *OsMADS34*/*PAP2* (*PANICLE PHYTOMER2*) together regulate determinacy of the floral meristem and specify the identities of spikelet organs by positively regulating the other MADS-box floral homeotic genes including B-, C-, *SEP3* and *AGL6* genes (Wu et al., 2017a).

In petunia sextuple *sep*/*agl6* mutant flowers, we found that the initial expression levels of the B-class genes *PhGLO1*, *PhGLO2* and *PhDEF* and of the C-class genes *PMADS3* and *FBP6* were comparable to WT, indicating that initial activation and expression of these genes does not depend on the *SEP*/*AGL6* floral organ identity function. In Arabidopsis, a similar observation has been made, showing normal patterning and accumulation of *AP3*, *PI* and *AG* expression in young *sep1 sep2 sep3* floral buds (Pelaz et al., 2000). With perhaps the exception of *FBP6* (*SHP1*/*2*), we found that further upregulation during later stages of development was impaired, especially for the *PI* homologs *PhGLO1* and *PhGLO2*, while *PhDEF* (*AP3*) and *PMADS3* (*AG*) still showed upregulation, but with a smaller incremental rate. These results are

724 in agreement with the idea that in Arabidopsis, complex formation of SEP proteins with B- and
725 C- class MADS-box proteins is required for their positive autoregulation (Gomez-Mena et al.,
726 2005; Kaufmann et al., 2009).

727 In sharp contrast with the other B-class genes, *PhTM6* expression levels in the sextuple
728 mutant were almost completely abolished during all stages tested, indicating a full dependence
729 on SEP/AGL6 activity for all stages of its expression. Earlier, we showed that regulation of
730 *PhTM6* expression is atypical for a B-class gene, since its expression largely depends on the
731 activity of the C-genes *PMADS3* and *FBP6* (Heijmans et al., 2012), resulting in a WT
732 expression pattern mainly in stamens and carpels from early developmental stages onwards,
733 and in all floral whorls when the C-genes are ectopically expressed (Vandenbussche et al.,
734 2004; Rijpkema et al., 2006). Together, this indicates that both *SEP* and C-class genes are
735 absolutely required for *PhTM6* expression, most likely as interaction partners in a MADS-box
736 protein complex (Ferrario et al., 2003). For *FBP11* (*STK*) expression, we found the same *SEP*
737 dependence, but since *FBP11* is expressed relatively late during flower development in the
738 developing placenta and ovules (Angenent et al., 1995), this may also be an indirect effect,
739 since these tissues are completely absent in the sextuple mutant. Thus, B- and C-class MADS-
740 box proteins may have an absolute requirement of SEP function to activate their downstream
741 developmental programs, but depend only partly on it for upregulation of their own expression.
742 This suggests differences in the molecular mechanisms involved in autoregulation versus
743 downstream target gene activation/repression.

744 Finally, we found that *UNS*, a petunia member of the *SOC1* family, was strongly
745 upregulated in the sextuple *sep*/*agl6* mutant from early stages onwards, suggesting that *SEP*
746 genes repress *UNS* during WT flower development. *SOC1* was identified as a direct target of
747 SEP3 in a genome wide study in Arabidopsis, with the expression of *SOC1* being already
748 reduced after only 8h of *SEP3* induction in seedlings (Kaufmann et al., 2009). Interestingly, it
749 was shown that constitutive *UNS* expression in petunia and Arabidopsis flowers lead to the
750 *unshaven* floral phenotype, which is characterized by ectopic trichome formation on floral
751 organs and conversion of petals into organs with leaf-like features (Ferrario et al., 2004). All
752 these observations are consistent with the finding of Ó'Maoiléidigh and colleagues, who
753 demonstrated that the floral homeotic organ identity gene *AG* not only functions by positively
754 conferring floral identity to organ primordia in the flower, but also by actively repressing
755 components of the leaf developmental program (OMaoileidigh et al., 2013).
756
757

The *FBP9* Subclade Genes together with a *SEP4-like Gene* are Required to Confer Floral Meristem Identity in petunia and tomato.

We found that the *FBP9* subclade members *FBP9* and *FBP23* together with *FBP4* play a crucial role in floral meristem identity, as illustrated by the homeotic transformation of flower meristems into inflorescence meristems in *fbp9 fbp23 fbp4* triple mutants. In contrast, genetic interactions with the *fbp2* mutant revealed only mild contributions to the classical *SEP* organ identity function. The phenotype of the *fbp9 fbp23 fbp4* triple mutant is strikingly similar to that of the floral meristem identity mutants *alf* and *dot* (Souer et al., 1998; Souer et al., 2008), but it remains to be investigated how these genes are hierarchically positioned. However, it was found that simultaneous overexpression of *ALF* and *DOT* in young seedlings led to strong activation of *FBP9* and *FBP23* expression (Souer et al., 2008), suggesting that ALF/DOT specify floral meristem identity at least in part by activating *FBP9* and *FBP23* expression. An expression analysis of *ALF*, *DOT*, *FBP9*, *FBP23* and *FBP4* in the different mutant backgrounds may provide further support for this hypothesis.

Importantly, our analysis of the *fbp4 fbp9 fbp23* mutant combined with a recent study of tomato *FBP9* and *SEP4* subclade members (Soyk et al., 2017) demonstrates that the requirement of *FBP9* and *SEP4* clade genes for floral meristem identity is conserved between tomato and petunia, and therefore likely also in other Solanaceous species. Note that although in both cases floral meristem identity is compromised, the phenotypes of tomato *j2 ej2 lin* and petunia *fbp9 fbp23 fbp4* mutants superficially do look quite different. We believe that this may be explained for an important part by basic differences in the inflorescence architecture between the two species. First of all, in petunia, every flower arises from a node that bears two bracts, while the tomato inflorescence is bractless. As a consequence, loss of FM identity in petunia leads to a highly branched structure composed of a lot of bracts, while in tomato this leads to a more naked structure consisting of proliferating SIMs. Also, the compound tomato inflorescence architecture is more complex compared to petunia and involves the transition of a vegetative meristem into a transition meristem (TM) that terminates in a floral meristem (FM) resulting in the first flower of the inflorescence. Additional flowers then develop from the axillary SIM, resulting in an inflorescence bearing multiple flowers (Park et al., 2014).

While the strongest phenotype was obtained in the tomato triple mutants, analysis of single and double mutants revealed also individual contributions to tomato development: *LIN* limits internode length and the number of flowers that develop per inflorescence, *EJ2* negatively regulates sepal size, while both *J2* and *EJ2* are involved in the control of branching

of the tomato inflorescence (Soyk et al., 2017). In addition, *J2* is required for the development of the pedicel abscission zone (Liu et al., 2014; Roldan et al., 2017; Soyk et al., 2017).

Finally, remark that our phylogenetic analysis indicates that within the *SEP4* clade, *RIN* in fact is more closely related to petunia *FBP4* compared to *LIN*. However, *RIN* shows a much more restricted expression pattern limited to the developing fruit (Vrebalov et al., 2002), indicating that *RIN* has evolved a specialized role compared to *FBP4 and LIN*. Because of the *rin* phenotype, *RIN* has long time been considered to function as a major regulator that is essential for the induction of ripening, but a recent study using a CRISPR/Cas9-mediated *RIN*-knockout mutation shows that inactivation of *RIN* does not repress initiation of ripening and that the original *rin* mutation is rather a gain-of-function mutation resulting in an aberrant protein that actively represses ripening (Ito et al., 2017).

While Arabidopsis doesn't have *FBP9* subclade members (Zahn et al., 2005), it was found that Arabidopsis SEP proteins, in addition to their role in floral organ identity, are also involved in maintaining floral meristem identity, as evidenced by the frequent appearance of secondary flowers in the axils of first-whorl organs in *sep1 sep2 sep3 sep4* quadruple mutants and much less frequently in *sep1 sep2 sep 3* mutants (Ditta et al., 2004). Moreover, an *ap1 sep1 sep2 sep4* quadruple mutant was shown to produce a *cauliflower* phenotype similar to *ap1 cal* mutants, while an *ap1 sep4* mutant had a meristem identity defect intermediate between that of *ap1* and *ap1 cal* mutants. Although these data clearly demonstrate the implication of Arabidopsis *SEP* genes in floral meristem identity, the very severe floral meristem defects observed in *ap1 cal* or *ap1 cal ful* mutants, indicate that in Arabidopsis, floral meristem is mainly determined by members of the *AP1*/*SQUA* subfamily.

In rice, the three *LOFSEP* genes *OsMADS1*/*LHS*, *OsMADS5*, and *OsMADS34*/*PAP2* were proposed to be involved in the transition of the spikelet meristem into a floral meristem (Wu et al., 2017a). However, floral meristem formation in the triple *osmads1 osmads5 osmads34* mutants was not completely abolished, only strongly delayed, possibly because the insertion alleles are not complete null mutants as suggested by the authors (Wu et al., 2017a).

The Petunia *AP1 ortholog euAP1 is* not required for petal development, and acts redundantly with the other *AP1* clade members as a B-function Repressor in the First Floral Whorl.

Because Arabidopsis *ap1* mutants lack petals and have sepals displaying bract like features (Irish and Sussex, 1990; Mandel et al., 1992) and *AP1* is negatively regulated by AG

in whorls three and four (Gustafson-Brown et al., 1994), *AP1* has been classified as an A-function gene in the ABC model, required for the identity specification of sepals and petals. In sharp contrast with the phenotype of Arabidopsis *ap1* mutants, we found that petal development does not at all require *euAP1* activity in petunia. This may not come as a complete surprise since it was shown before that also in Arabidopsis, *AP1* is not essential for petal development, as evidenced by the nearly complete restauration of petal development in *ap1 ag* mutants (Bowman et al., 1993) and in *35S: SEP3 ap1* flowers (Castillejo et al., 2005), and a partial restauration in *ap1 agl24* double mutants (Yu et al., 2004). In addition, single *euap1* mutants that still develop petals have previously been described in other species such as e.g. the *squa* mutant in snapdragon (Huijser et al., 1992), the *pim* mutant in pea (Berbel et al., 2001; Taylor et al., 2002), *mtap1* in *Medicago* (Benlloch et al., 2006; Cheng et al., 2018), and *mc* in tomato (Vrebalov et al., 2002; Nakano et al., 2012; Yuste-Lisbona et al., 2016).

Restricting the activity of the floral homeotic B- and C-functions to their proper domains is crucial for the correct development of the flower structure, and it appears that the molecular mechanisms underlying these cadastral functions are much more diverse compared to the floral organ identity functions (reviewed in (Monniaux and Vandenbussche, 2018)). Here we identified the petunia *AP1*/*SQUA* genes as repressors of the B-function in the first whorl, as evidenced by the partial conversion of sepals into petaloid tissue in *pfg fbp26 fbp29 euap1* mutants, and the strong enhancement of this phenotype in combination with mutations in the *ROB* genes, which were previously identified as B-function repressors in the first whorl (Morel et al., 2017). Such a phenotype has so far never been reported in flowers of Arabidopsis *ap1*, *cal* or *ful* mutants, or any combination of these mutations (Ferrandiz et al., 2000). Nevertheless, it was proposed that *AP1* in combination with *AGL24* (*AGAMOUS LIKE 24*) and *SVP* (*SHORT VEGETATIVE PHASE*) represses both the B- and C-function genes during early phases of floral development (Gregis et al., 2006; Gregis et al., 2009), but it is not clear if other Arabidopsis *AP1*/*SQUA* genes would be also involved in this process and whether this is specific to the first floral whorl. Finally in rice, deregulation of B- and C-expression patterns was observed in *osmads14 osmads15*/+ and osmads14/+ osmads15 flowers (Wu et al., 2017b), suggesting that these rice AP1/SQUA transcription factors are also involved in patterning the homeotic B- and C-functions.

In summary, the observation that the petunia *AP1*/*SQUA* genes repress the B-function in the first floral whorl but do not seem to be required for 2nd whorl petal development demonstrates that petunia *AP1*/*SQUA* genes cannot be easily classified as “A-function” genes according to the original definition of the A-function in the ABC model. Earlier, we

encountered the same difficulties when trying to integrate the function of the petunia *AP2*-like transcription factors *AP2* and *ROB1-3* into a simple ABC model (Morel et al., 2017). This led us to propose a modified model for petunia floral organ identity in which the original A-function is replaced by a combinatorial function describing the cadastral (boundary setting) mechanisms that pattern the floral B- and C-functions (Morel et al., 2017). The above described cadastral function of the petunia *AP1*/*SQUA* genes during flower development perfectly fits into this alternative model, and is also compatible with the proposed modified (A)BC model (Causier et al., 2009), in which a more broadly defined (A)-function provides the genetic context in which the B- and C-functions are active and regulates both their spatial and temporal expression domains. Our findings for both the *AP1*/*SQUA* and *AP2-like* gene functions in petunia entirely explain the struggles to translate the Arabidopsis definition of the A-function to distant flowering species (Litt, 2007).

Petunia *AP1*/*SQUA* Family Members Function in a Largely Redundant Fashion and are Required for Inflorescence Meristem Identity.

Different members of the *AP1*/*SQUA* subfamily in Arabidopsis have evolved unique roles during development as exemplified by the distinct phenotypes of the single *ap1* and *ful* mutants. Swapping experiments suggest that functional divergence between *AP1* and *FUL* is due to changes in both expression pattern and coding sequence (McCarthy et al., 2015). At the same time, *AP1*, *CAL* and *FUL* have retained a redundant function in inflorescence architecture (Ferrandiz et al., 2000), whereas *CAL* shares a cryptic role in petal development redundantly with *AP1* (Castillejo et al., 2005). While the function of *AGL79* (a *euFUL*-like gene) has remained elusive for a long time, a recent study suggests a role for *AGL79* in lateral root development and control of lateral shoot branching (Gao et al., 2017). It remains to be established if *AGL79* overlaps in function with *AP1*, *CAL* and *FUL*.

Although we cannot exclude to have overlooked some very subtle defects, the absence of clear floral developmental defects in mutants for any of the four petunia *AP1*/*SQUA* genes suggests that individual members of the petunia *AP1*/*SQUA* subfamily did not functionally diverge, independent from their *euAP1* or *euFUL*/*paleoAP1* clade identity. In line with that, we found that all four genes show overlapping expression patterns in most tissues tested. It remains to be tested whether this broad functional redundancy is also observed during other developmental processes, such root or fruit development, which were not analyzed in this study.

One of the striking aspects of the phenotype of quadruple *pfg fbp26 fbp29 euap1* mutants is that these plants develop fully functional flowers, suggesting that floral meristem identity

does not require AP1/SQUA activity in petunia. Our finding that this function is apparently taken care off by a specific subset of *SEP* genes fully fits this hypothesis. However, we can currently not fully exclude that some residual AP1/SQUA activity remains in the *pfg fbp26 fbp29 euap1* mutants, possibly explaining the formation of terminal flowers. Especially the *pfg-12* insertion allele potentially could be a hypomorphic allele, since an alternative startcodon is present in the first exon (AA nr 8, Supplemental Data File 2) shortly after the transposon insertion site. This could in theory lead to the production of a protein with an N-terminal truncation of the MADS-domain, perhaps displaying some residual functionality. Other alleles will have to be identified in the future to fully proof the hypothesis that floral meristem identity in petunia does not require AP1/SQUA activity.

On the other hand, the phenotype of the quadruple *pfg fbp26 fbp29 euap1* mutants indicate that the petunia *AP1*/*SQUA* genes appear to be essential for the development of the cymose inflorescence, indicating a role in inflorescence meristem identity. Such a role also has been proposed for *AP1*/*SQUA* genes in other core eudicot species: *VEG1* and its ortholog *MtFUL* are essential for the specification of the secondary inflorescence meristem in the compound inflorescences of pea and *Medicago* respectively, but are not required for floral meristem identity (Berbel et al., 2012; Cheng et al., 2018).

Interestingly, it was earlier found that the tomato *mc* mutants also play a role in inflorescence meristem development, since *mc* inflorescences revert to vegetative growth after forming two to three flowers. In addition, these flowers developed enlarged sepals and have an incomplete pedicel abscission zone (Vrebalov et al., 2002; Nakano et al., 2012; Yuste-Lisbona et al., 2016). Moreover, the implication of MC in the development of the pedicel abscission zone is proposed to occur via a higher order MADS-box complex including the SVP-like protein JOINTLESS (J), and J2/SLMBP21 a SEP FBP9 clade member . Except for the pedicel abscission zone which does not exist in petunia, the *mc* phenotypes are reminiscent of what we observed in petunia quadruple *ap1* mutants, suggesting a conserved role in inflorescence meristem identity and first whorl development. Because *mc* single mutants have a clear phenotype on their own, it also shows that *MC* exhibits less functional overlap with the other *AP1* family members compared to petunia. However, as suggested by the relative mildness of the inflorescence meristem defect in *mc* mutants compared to the petunia quadruple mutants, this does not exclude possible partial redundancy with one or more of the other tomato *AP1* family members, something that still remains to be tested. RNAi mediated downregulation of tomato *FUL1* and *FUL2* suggested a role for these genes in fleshy fruit ripening (Bemer et al., 2012; Shima et al., 2013; Wang et al., 2014), indicating that the implication of *FUL* genes in

fruit development is conserved between tomato and Arabidopsis, despite that these two species have very different fruit types (fleshy versus dry). Petunia on the other hand develops a dry fruit capsule, but the implication of *AP1*/*FUL* members in its development remains to be investigated.

Finally, of the four identified rice *AP1* subfamily members called *OsMADS14*, *OsMADS15*, *OsMADS18* and *OsMADS20* (Lee et al., 2003; Yu et al., 2016), it was found that *OsMADS14*, *OsMADS15* and *OsMADS18* are specifically activated in the meristem at phase transition together with the *LOFSEP* gene *PAP2*/*OsMADS34* (Kobayashi et al., 2010; Kobayashi et al., 2012). While downregulation of these three *AP1*/*FUL-like* genes by RNAi caused only a slight delay in reproductive transition, further depletion of *PAP2* function from these triple knockdown plants inhibited the transition of the meristem to the IM (Kobayashi et al., 2012), indicating that the *AP1*/*FUL-like OsMADS14*, *OsMADS15*, *OsMADS18* and the *LOFSEP* gene *PAP2*/*OsMADS34* coordinately act in the meristem to specify inflorescence meristem identity. In addition, it was shown that *OsMADS14* and *OsMADS15*, besides to their function of specifying meristem identity, are also involved in the specification of palea and lodicule identities, using stable mutant alleles (Wu et al., 2017b).

Functional Diversification Patterns in the *AP1*/*SEP*/*AGL6* Superclade during Angiosperm evolution.

Above, we compared *AP1*/*SEP*/*AGL6* functions between different species, mainly focusing on Arabidopsis, petunia, tomato and rice, revealing important differences in the functions performed by their respective members. Perhaps the most striking observation is that a subclass of *SEP* genes (all belonging to the *LOFSEP* group) in petunia, tomato and possibly also rice are required to confer floral meristem identity, while in Arabidopsis the floral meristem identity function is mainly associated with members of the *AP1*/*SQUA* subfamily. It thus seems that during angiosperm evolution, members of different subfamilies within the *AP1*/*SEP*/*AGL6* superclade have evolved specialized/subfunctionalized roles either in floral organ identity or inflorescence and/or floral meristem determination, providing further genetic support for the monophyletic origin of the *AP1*/*SEP*/*AGL6* superclade. Within MADS-box subfamilies, it is not unusual that functions have been distributed differently between paralogs in different species. One of the first well documented cases concerns the C-function MADS-box subfamily, showing that the canonical C-function is encoded by nonorthologous genes in Arabidopsis and Antirrhinum (Causier et al., 2005). However, careful comparison of gene functions in the AP1/SEP/AGL6 superclade suggest that this random distribution of functions after gene

duplication has occurred also during the earlier phases of the evolution of the MADS-box gene family, resulting in functions that are differently distributed beyond the subfamily level. In addition, comparison between tomato and petunia indicates major functional differences that have arisen on a relatively short evolutionary time-scale. Of note is the involvement of several tomato *AP1*/*SEP*/*AGL6* members in the development of the pedicel abscission zone and in compound leaf development, all processes that do not occur in petunia.

Together, these observations illustrate that gene function cannot accurately be predicted solely based on sequence homology and phylogenetic analysis, and that final gene function may be strongly dependent on species-specific developmental contexts. Furthermore, it also illustrates that demonstration of gene function conservation between only two species, even if they are very distantly related (e.g. a monocot versus a dicot species), cannot safely be used to extrapolate a more general conservation of a particular gene function. Together with other studies, this further enforces the argument that plant biology in general, and plant evo–devo in particular would strongly benefit from a broader range of available model systems (Vandenbussche et al., 2016).

MATERIALS AND METHODS

Plant Material, Genotyping and Phenotyping

Petunia plants were grown in soil (FAVORIT-argile 10) either in a greenhouse (16 h day/8 h night: natural light supplemented with Philips Sodium HPS 400W SON-T AGRO light bulbs; 55.000 lumens) or outside protected by an agricultural tunnel (from April to October), both under conditions that depend on local seasonal changes (45.72°N 4.82°E), or in growth chambers (settings: 16 h day 22°C /8 h night 18°C, 75W Valoya NS12 LED bars, light intensity 130 μE). The identification of the following *dTph1* transposon insertion alleles (Figures 1G and 5D) was described previously (current allele naming based on exact insert position; old allele names in between brackets): *fbp2-332* (*fbp2-1*); *fbp2-440* (*fbp2-2*); *fbp4-44* (*fbp4-2*); *fbp4-55* (*fbp4-3*); *fbp5-129* (*fbp5-1*); *fbp9-110* (*fbp9-1*); *pfg-12* (*pfg-1*); *fbp26-76* (*fbp26-1*) (Vandenbussche et al., 2003b), and *agl6-118* (*agl6-1*) (Rijpkema et al., 2009). Note that the previously determined insert positions for some of these alleles differ by a few nucleotides compared to the data presented here, due to the imperfect manual sequencing method used at that time combined with the characterization of only the right border of the transposon flanking sequences, not taking the *dTph1* 8bp target site duplication into account. Also, it was mentioned that homozygous *fbp9-1* (*fbp9-110*) mutants exhibited aberrations in plant architecture during the reproductive phase (Vandenbussche et al., 2003b). However, later outcrossing analysis of

the *fbp9-1* allele showed that this defect was closely linked to *fbp9-1*, but not due to the *fbp9-1* insertion, as confirmed by the absence of this phenotype in the new *fbp9-7* and *fbp9-90* alleles. The following alleles *fbp2-209*; *fbp4-23*; *fbp5-51*; *pm12-37*; *pm12-118*; *pm12-325*; *euap1-317*; *fbp29-31*; *fbp29-123* and *fbp29-153* were identified by BLAST-searching our sequence-indexed *dTph1* transposon flanking sequence database (Vandenbussche et al., 2008) that was enlarged with the addition of extra populations. Exact insert positions were determined by aligning the transposon flanking sequences with the corresponding genomic and coding sequences. The insertion alleles were named after their exact insert position, expressed in bp downstream of the ATG in the coding sequence (Figures 1G and 5D). Offspring of candidate insertion lines were grown and genotyped by PCR using gene specific primer pairs flanking the insertion site (Supplemental Table 2). The following thermal profile was used for segregation analysis PCR: 11 cycles (94°C for 15s, 71°C for 20s minus 1°C/cycle, 72°C for 30s), followed by 40 cycles (94°C for 15s, 60°C for 20s, 72°C for 30s). For all alleles, homozygous mutants were obtained in offspring of the originally heterozygous insertion mutants, either containing the original transposon insertion allele, or a stably inherited out-of-frame derived footprint allele that was confirmed by sequencing, fully maintaining the mutation. Insertion alleles that were used in crosses for higher order mutant analysis are indicated in red in Figures 1G and 5D. The different insertion alleles were further systematically genotyped in subsequent crosses and segregation analyses. To test genetic interactions with the *rob* mutations (Figure 6), a *pfg fbp26 fbp29 euap1* mutant was crossed with the earlier described *rob1 rob2 rob3* mutant (Morel et al., 2017). Phenotypic analysis of all single and higher order mutants was focused and limited to the screening for defects in floral organ development and inflorescence architecture.

Phylogenetic Analysis

The phylogenetic analyses shown in Figures 1F and 5A were conducted using the advanced PhyML/oneClick workflow at ngphylogeny.fr (Lemoine et al., 2019). Full-length protein sequences of either SEP/AGL6 (Figure 1F) or AP1/SQUA (Figure 5A) subfamily members from petunia, tomato, arabidopsis and rice (Supplemental Table 1) were first aligned using MAFFT (Katoh and Standley, 2013) applying the following options: Data type: Autodetection; MAFFT flavor: auto; Gap extend penalty: 0.123; Gap opening penalty: 1.53; Matrix selection: no matrix; Reorder output? true. Output format: FASTA (Supplemental Data files 1 and 2). Next, alignment curation was done using BMGE (Criscuolo and Gribaldo, 2010) with the following options: Sequence coding: AA; matrix: BLOSUM; Estimated matrix BLOSUM: 62; Sliding windows size: 3; Maximum entropy threshold: 0.5; Gap Rate cut-off: 0.5; Minimum

block size: 3 and 5 for Figures 1F and 5A respectively. Using the resulting BMGE files, Maximum Likelyhood trees were calculated using PhyML (Lemoine et al., 2018) with the following settings: Data type: amino acids; Evolutionary model: LG; Equilibrium frequencies: ML/Model. Proportion of invariant sites: estimated; Number of categories for the discrete gamma model: 4; Parameter of the gamma model: estimated; Tree topology search: Best of NNI and SPR. Optimize parameter: Tree topology, Branch length, Model parameter; Statistical test for branch support: Bootstrap; Number of bootstrap replicates: 1000. Seed value used to initiate the random number generator: 123456. The tree was rendered using Newick Display (Junier and Zdobnov, 2010). For the visual representation of the SEP/AGL6 analysis (Figure 1F), mid-point rooting was applied on the node separating SEP and AGL6 subfamilies, while for the AP1/SQUA analysis (Figure 5A), mid-point rooting was applied on the node separating rice from eudicot AP1/SQUA proteins.

Imaging and Microscopy

Electron microscopy images were obtained as previously described (Vandenbussche et al., 2009) or by using a HIROX SH-1500 benchtop environmental electron microscope equipped with a cooled stage. Macroscopic floral phenotypes were imaged by conventional digital photography using a glass plate as a support and black velvet tissue around 10 cm below the glass plate in order to generate a clean black background. When needed, backgrounds were further equalized by removing dust particles and light reflections with Photoshop. Images in Figures 6H, 6I and 6M were photographed using a Zeiss Imager M2 microscope equipped with an AxioCam MRc camera (Zeiss).

RT-qPCR Expression Analysis.

Total RNA was extracted using the Spectrum Plant Total RNA kit (Sigma Aldrich) and treated with Turbo DNA-free DNase I (Ambion). RNA was reverse transcribed using RevertAid M-MuLV reverse transcriptase (Fermentas) according to the manufacturer's protocol. PCR reactions were performed in an optical 384-well plate in the QuantStudio™ 6 Flex Real-Time PCR System (Applied Biosystems), using FastStart Universal SYBR Green Master (Roche), in a final volume of 10µl, according to the manufacturer's instructions. Primers (Supplemental Table 2) were designed using the online Universal ProbeLibrary Assay Design Center (Roche). Data were analyzed using the QuantStudio™ 6 and 7 Flex Real-Time PCR System Software v1.0 (Applied Biosystems). Petunia *ACTIN*, *GAPDH*, and *RAN* were used as reference genes. PCR efficiency (*E*) was estimated from the data obtained from standard curve amplification

using the equation $E=10^{-1/\text{slope}}$. Relative expression (R.E.) values on the *y*-axes are the average of nine data points resulting from the technical triplicates of three biological replicates ± sd and normalized to the geometrical average of three $E^{-\Delta Ct}$, where $\Delta Ct = Ct_{GOI} - Ct_{ACTIN,\ GAPDH \text{ and } RAN}$.

The floral bud series (marked floral buds 1–3 in Figures 1F, 4G, 5C and Supplemental Figure 1) are successive developmental stages of complete floral buds harvested from the same inflorescences (Figure 1E). Young bracts were harvested from the node bearing stage 3 flowers, while inflorescence stem tissue was collected from the internode connecting node stage 4 and stage 5 bearing flowers. For each biological replicate, corresponding stages harvested from three inflorescences were pooled. Stage 3 corresponds to flower buds with a diameter of ~5 mm and from which individual floral organs can be easily dissected by hand. All analyses showing expression in separate floral organ types are from this stage. Biological replicates of the different floral organ types were composed of pooled stage 3 organs harvested from three different flowers each time. Floral buds marked "2" (diameter ~2.5 mm) and "1" (diameter ~1.5 mm) are younger stages and were harvested from the next two nodes produced after bud stage 3. In addition to 1.5-mm buds, stage 1 also includes the inflorescence meristem and very young developing floral primordia subtended by bracts, which are attached to the base of the pedicel of the 1.5-mm bud. For the sextuple mutant flower buds analyzed in Figure 4G, developmental stages in relation to wild-type development were deduced based on their position on the inflorescence. Vegetative apices (including very small leaf primordia) were harvested from 3-week-old seedlings by manually removing cotyledons, roots, and developed leaves. Young leaf primordia were isolated from the same 3-week-old seedlings. Each biological replicate of the vegetative apices and young leaf primordia consisted of pooled material harvested from each time 10 seedlings. The root samples were obtained by pooling 10-15 actively growing 2 cm root tips per biological replicate.

Accession Numbers

Sequence data for the genes that were functionally analyzed in this article can be found in the GenBank/EMBL libraries under accession numbers *FBP2* (M91666.1); *FBP5* (AF335235.1); *PMADS12* (AY370527.1); *FBP9* (AF335236.1); *FBP23* (AF335241.1); *FBP4* (AF335234.1); *Ph-AGL6* (AB031035.1); *PFG* (AF176782.1); *FBP29* (AF335245.1); *FBP26* (AF176783.1); *Ph-euAP1* (MK598839) (see also Supplemental Table 1).

Supplemental Data

Supplemental Figure 1. RT-qPCR Expression Analysis of the Petunia *UNSHAVEN* (*UNS*) Gene in WT.

Supplemental Figure 2. Further Characterization of the Petunia *AP1*/*SQUA* family.

Supplemental Table 1. Gene Names, Synonyms and Accession Codes/Gene Models for Sequences Shown in Figures 1 and 5, in Supplemental Figures 2, and in Supplemental Data Files 1, 2, 3, and 4.

Supplemental Table 2. Oligo Sequences Used in this Study.

Supplemental Data File 1: MAFFT Multiple Alignment of SEP and AGL6 Protein Sequences from Petunia (Ph), Tomato (Sl), Arabidopsis (At) and Rice (Os) in fasta format.

Supplemental Data File 2: MAFFT Multiple Alignment of AP1/SQUA Protein Sequences from Petunia (Ph), Tomato (Sl), Arabidopsis (At) and Rice (Os) in fasta format.

Supplemental Data File 3: SEP/AGL6 Newick tree file.

Supplemental Data File 4: AP1/SQUA Newick tree file.

Acknowledgments

M.V. was supported by a CNRS ATIP-AVENIR award and the French National Research Agency program DODO (ANR-16CE20-0024-03). We thank A. Lacroix, J. Berger and P. Bolland for plant care assistance, and V. Bayle for electron microscopy technical support performed at the PLATIM platform, IFR BioScience Lyon (UMS3444/US8). We thank A. Rijpkema for help with preliminary studies.

Author Contributions

M.V. and P.M. conceived and designed the experiments. P.M., P.C., V.B. S.C., F.R., S.R.B., C.T., J.Z., and M.V. performed the experiments. P.M. and M.V. analyzed the data. M.V., M.M. and P.M. wrote the manuscript.

REFERENCES

Agrawal, G.K., Abe, K., Yamazaki, M., Miyao, A., and Hirochika, H. (2005). Conservation of the E-function for floral organ identity in rice revealed by the analysis of tissue

culture-induced loss-of-function mutants of the OsMADS1 gene. Plant Mol Biol **59,** 125-135.

Angenent, G.C., Franken, J., Busscher, M., Colombo, L., and van Tunen, A.J. (1993). Petal and stamen formation in petunia is regulated by the homeotic gene fbp1. The Plant Journal **4,** 101-112.

Angenent, G.C., Franken, J., Busscher, M., Weiss, D., and van Tunen, A.J. (1994). Co-suppression of the petunia homeotic gene fbp2 affects the identity of the generative meristem. Plant J **5,** 33-44.

Angenent, G.C., Franken, J., Busscher, M., van Dijken, A., van Went, J.L., Dons, H., and van Tunen, A.J. (1995). A Novel Class of MADS Box Genes Is Involved in Ovule Development in Petunia. Plant Cell **7,** 1569-1582.

Becker, A., and Theissen, G. (2003). The major clades of MADS-box genes and their role in the development and evolution of flowering plants. Mol Phylogenet Evol **29,** 464-489.

Bemer, M., Karlova, R., Ballester, A.R., Tikunov, Y.M., Bovy, A.G., Wolters-Arts, M., Rossetto Pde, B., Angenent, G.C., and de Maagd, R.A. (2012). The tomato FRUITFULL homologs TDR4/FUL1 and MBP7/FUL2 regulate ethylene-independent aspects of fruit ripening. Plant Cell **24,** 4437-4451.

Benlloch, R., d'Erfurth, I., Ferrandiz, C., Cosson, V., Beltran, J.P., Canas, L.A., Kondorosi, A., Madueno, F., and Ratet, P. (2006). Isolation of mtpim proves Tnt1 a useful reverse genetics tool in Medicago truncatula and uncovers new aspects of AP1-like functions in legumes. Plant Physiol **142,** 972-983.

Berbel, A., Navarro, C., Ferrandiz, C., Canas, L.A., Madueno, F., and Beltran, J.P. (2001). Analysis of PEAM4, the pea AP1 functional homologue, supports a model for AP1-like genes controlling both floral meristem and floral organ identity in different plant species. Plant J **25,** 441-451.

Berbel, A., Ferrandiz, C., Hecht, V., Dalmais, M., Lund, O.S., Sussmilch, F.C., Taylor, S.A., Bendahmane, A., Ellis, T.H., Beltran, J.P., Weller, J.L., and Madueno, F. (2012). VEGETATIVE1 is essential for development of the compound inflorescence in pea. Nat Commun **3,** 797.

Bombarely, A., Moser, M., Amrad, A., Bao, M., Bapaume, L., Barry, C.S., Bliek, M., Boersma, M.R., Borghi, L., Bruggmann, R.m., Bucher, M., D'Agostino, N., Davies, K., Druege, U., Dudareva, N., Egea-Cortines, M., Delledonne, M., Fernandez-Pozo, N., Franken, P., Grandont, L., Heslop-Harrison, J.S., Hintzsche, J., Johns, M., Koes, R., Lv, X., Lyons, E., Malla, D., Martinoia, E., Mattson, N.S., Morel, P., Mueller, L.A., Muhlemann, J.l., Nouri, E., Passeri, V., Pezzotti, M., Qi, Q., Reinhardt, D., Rich, M., Richert-P√∂ggeler, K.R., Robbins, T.P., Schatz, M.C., Schranz, M.E., Schuurink, R.C., Schwarzacher, T., Spelt, K., Tang, H., Urbanus, S.L., Vandenbussche, M., Vijverberg, K., Villarino, G.H., Warner, R.M., Weiss, J., Yue, Z., Zethof, J., Quattrocchio, F., Sims, T.L., and Kuhlemeier, C. (2016). Insight into the evolution of the Solanaceae from the parental genomes of Petunia hybrida. Nature Plants **2,** 16074.

Bowman, J.L., Smyth, D.R., and Meyerowitz, E.M. (1991). Genetic interactions among floral homeotic genes of Arabidopsis. Development **112,** 1-20.

Bowman, J.L., Smyth, D.R., and Meyerowitz, E.M. (2012). The ABC model of flower development: then and now. Development **139,** 4095-4098.

Bowman, J.L., Alvarez, J., Weigel, D., Meyerowitz, E.M., and Smyth, D.R. (1993). Control of flower development in Arabidopsis thaliana by APETALA1 and interacting genes. Development **119,** 721-743.

Burko, Y., Shleizer-Burko, S., Yanai, O., Shwartz, I., Zelnik, I.D., Jacob-Hirsch, J., Kela, I., Eshed-Williams, L., and Ori, N. (2013). A role for APETALA1/fruitfull transcription factors in tomato leaf development. Plant Cell **25,** 2070-2083.

Cartolano, M., Castillo, R., Efremova, N., Kuckenberg, M., Zethof, J., Gerats, T., Schwarz-Sommer, Z., and Vandenbussche, M. (2007). A conserved microRNA module exerts homeotic control over Petunia hybrida and Antirrhinum majus floral organ identity. Nature Genetics **39,** 901-905.

Castel, R., Kusters, E., and Koes, R. (2010). Inflorescence development in petunia: through the maze of botanical terminology. J Exp Bot **61,** 2235-2246.

Castillejo, C., Romera-Branchat, M., and Pelaz, S. (2005). A new role of the Arabidopsis SEPALLATA3 gene revealed by its constitutive expression. Plant J **43,** 586-596.

Causier, B., Schwarz-Sommer, Z., and Davies, B. (2009). Floral organ identity: 20 years of ABCs. Seminars in Cell & Developmental Biology **21,** 73-79.

Causier, B., Castillo, R., Zhou, J., Ingram, R., Xue, Y., Schwarz-Sommer, Z., and Davies, B. (2005). Evolution in Action: Following Function in Duplicated Floral Homeotic Genes. Current Biology **15,** 1508-1512.

Chen, Z.X., Wu, J.G., Ding, W.N., Chen, H.M., Wu, P., and Shi, C.H. (2006). Morphogenesis and molecular basis on naked seed rice, a novel homeotic mutation of OsMADS1 regulating transcript level of AP3 homologue in rice. Planta **223,** 882-890.

Cheng, X., Li, G., Tang, Y., and Wen, J. (2018). Dissection of genetic regulation of compound inflorescence development in Medicago truncatula. Development **145**.

Coen, E.S., and Meyerowitz, E.M. (1991). The war of the whorls: genetic interactions controlling flower development. Nature **353,** 31-37.

Coen, E.S., Romero, J.M., Doyle, S., Elliott, R., Murphy, G., and Carpenter, R. (1990). floricaula: a homeotic gene required for flower development in antirrhinum majus. Cell **63,** 1311-1322.

Colombo, L., Battaglia, R., and Kater, M.M. (2008). Arabidopsis ovule development and its evolutionary conservation. Trends Plant Sci **13,** 444-450.

Colombo, L., Franken, J., Koetje, E., van Went, J., Dons, H., Angenent, G.C., and van Tunen, A.J. (1995). The Petunia MADS box gene FBP11 determines ovule identity. Plant Cell **7,** 1859-1868.

Criscuolo, A., and Gribaldo, S. (2010). BMGE (Block Mapping and Gathering with Entropy): a new software for selection of phylogenetic informative regions from multiple sequence alignments. BMC Evol Biol **10,** 210.

Cui, R., Han, J., Zhao, S., Su, K., Wu, F., Du, X., Xu, Q., Chong, K., Theissen, G., and Meng, Z. (2010). Functional conservation and diversification of class E floral homeotic genes in rice (Oryza sativa). Plant J **61,** 767-781.

Ditta, G., Pinyopich, A., Robles, P., Pelaz, S., and Yanofsky, M.F. (2004). The SEP4 gene of Arabidopsis thaliana functions in floral organ and meristem identity. Curr Biol **14,** 1935-1940.

Dreni, L., and Zhang, D. (2016). Flower development: the evolutionary history and functions
of the AGL6 subfamily MADS-box genes. J Exp Bot **67,** 1625-1638.

Egea-Cortines, M., Saedler, H., and Sommer, H. (1999). Ternary complex formation between the MADS-box proteins SQUAMOSA, DEFICIENS and GLOBOSA is involved in the control of floral architecture in Antirrhinum majus. EMBO J **18,** 5370-5379.

Favaro, R., Pinyopich, A., Battaglia, R., Kooiker, M., Borghi, L., Ditta, G., Yanofsky, M.F., Kater, M.M., and Colombo, L. (2003). MADS-box protein complexes control carpel and ovule development in Arabidopsis. Plant Cell **15,** 2603-2611.

Ferrandiz, C., Gu, Q., Martienssen, R., and Yanofsky, M.F. (2000). Redundant regulation of meristem identity and plant architecture by FRUITFULL, APETALA1 and CAULIFLOWER. Development **127,** 725-734.

Ferrario, S., Immink, R.G., Shchennikova, A., Busscher-Lange, J., and Angenent, G.C. (2003). The MADS box gene FBP2 is required for SEPALLATA function in petunia. Plant Cell **15,** 914-925.

Ferrario, S., Busscher, J., Franken, J., Gerats, T., Vandenbussche, M., Angenent, G.C., and Immink, R.G. (2004). Ectopic expression of the petunia MADS box gene UNSHAVEN accelerates flowering and confers leaf-like characteristics to floral organs in a dominant-negative manner. Plant Cell **16,** 1490-1505.

Gao, R., Wang, Y., Gruber, M.Y., and Hannoufa, A. (2017). miR156/SPL10 Modulates Lateral Root Development, Branching and Leaf Morphology in Arabidopsis by Silencing AGAMOUS-LIKE 79. Front Plant Sci **8,** 2226.

Gomez-Mena, C., de Folter, S., Costa, M.M., Angenent, G.C., and Sablowski, R. (2005). Transcriptional program controlled by the floral homeotic gene AGAMOUS during early organogenesis. Development **132,** 429-438.

Gregis, V., Sessa, A., Colombo, L., and Kater, M.M. (2006). AGL24, SHORT VEGETATIVE PHASE, and APETALA1 Redundantly Control AGAMOUS during Early Stages of Flower Development in Arabidopsis. Plant Cell **18,** 1373-1382.

Gregis, V., Sessa, A., Dorca-Fornell, C., and Kater, M.M. (2009). The Arabidopsis floral meristem identity genes AP1, AGL24 and SVP directly repress class B and C floral homeotic genes. Plant J **60,** 626-637.

Gu, Q., Ferrandiz, C., Yanofsky, M., and Martienssen, R. (1998). The FRUITFULL MADS-box gene mediates cell differentiation during Arabidopsis fruit development. Development **125,** 1509-1517.

Gustafson-Brown, C., Savidge, B., and Yanofsky, M.F. (1994). Regulation of the arabidopsis floral homeotic gene APETALA1. Cell **76,** 131-143.

Heijmans, K., Ament, K., Rijpkema, A.S., Zethof, J., Wolters-Arts, M., Gerats, T., and Vandenbussche, M. (2012). Redefining C and D in the Petunia ABC. Plant Cell **24,** 2305-2317.

Honma, T., and Goto, K. (2001). Complexes of MADS-box proteins are sufficient to convert leaves into floral organs. Nature **409,** 525-529.

Hsu, W.H., Yeh, T.J., Huang, K.Y., Li, J.Y., Chen, H.Y., and Yang, C.H. (2014). AGAMOUS-LIKE13, a putative ancestor for the E functional genes, specifies male and female gametophyte morphogenesis. Plant J **77,** 1-15.

Huang, X., Effgen, S., Meyer, R.C., Theres, K., and Koornneef, M. (2012). Epistatic natural allelic variation reveals a function of AGAMOUS-LIKE6 in axillary bud formation in Arabidopsis. Plant Cell **24,** 2364-2379.

Huijser, P., Klein, J., Lonnig, W.E., Meijer, H., Saedler, H., and Sommer, H. (1992). Bracteomania, an inflorescence anomaly, is caused by the loss of function of the MADS-box gene squamosa in Antirrhinum majus. EMBO J **11,** 1239-1249.

Immink, R.G., Gadella, T.W., Jr., Ferrario, S., Busscher, M., and Angenent, G.C. (2002). Analysis of MADS box protein-protein interactions in living plant cells. Proc Natl Acad Sci U S A **99,** 2416-2421.

Immink, R.G., Ferrario, S., Busscher-Lange, J., Kooiker, M., Busscher, M., and Angenent, G.C. (2003). Analysis of the petunia MADS-box transcription factor family. Mol Genet Genomics **268,** 598-606.

Immink, R.G., Hannapel, D.J., Ferrario, S., Busscher, M., Franken, J., Lookeren Campagne, M.M., and Angenent, G.C. (1999). A petunia MADS box gene involved

in the transition from vegetative to reproductive development. Development **126,** 5117-5126.

Immink, R.G., Tonaco, I.A., de Folter, S., Shchennikova, A., van Dijk, A.D., Busscher-Lange, J., Borst, J.W., and Angenent, G.C. (2009). SEPALLATA3: the 'glue' for MADS box transcription factor complex formation. Genome Biol **10,** R24.

Irish, V.F., and Sussex, I.M. (1990). Function of the apetala-1 gene during Arabidopsis floral development. Plant Cell **2,** 741-753.

Ito, Y., Nishizawa-Yokoi, A., Endo, M., Mikami, M., Shima, Y., Nakamura, N., Kotake-Nara, E., Kawasaki, S., and Toki, S. (2017). Re-evaluation of the rin mutation and the role of RIN in the induction of tomato ripening. Nat Plants **3,** 866-874.

Jeon, J.S., Jang, S., Lee, S., Nam, J., Kim, C., Lee, S.H., Chung, Y.Y., Kim, S.R., Lee, Y.H., Cho, Y.G., and An, G. (2000). leafy hull sterile1 is a homeotic mutation in a rice MADS box gene affecting rice flower development. Plant Cell **12,** 871-884.

Junier, T., and Zdobnov, E.M. (2010). The Newick utilities: high-throughput phylogenetic tree processing in the UNIX shell. Bioinformatics **26,** 1669-1670.

Kapoor, M., Tsuda, S., Tanaka, Y., Mayama, T., Okuyama, Y., Tsuchimoto, S., and Takatsuji, H. (2002). Role of petunia pMADS3 in determination of floral organ and meristem identity, as revealed by its loss of function. The Plant Journal **32,** 115-127.

Kater, M.M., Colombo, L., Franken, J., Busscher, M., Masiero, S., Van Lookeren Campagne, M.M., and Angenent, G.C. (1998). Multiple AGAMOUS Homologs from Cucumber and Petunia Differ in Their Ability to Induce Reproductive Organ Fate. Plant Cell **10,** 171-182.

Katoh, K., and Standley, D.M. (2013). MAFFT multiple sequence alignment software version 7: improvements in performance and usability. Mol Biol Evol **30,** 772-780.

Kaufmann, K., Muino, J.M., Jauregui, R., Airoldi, C.A., Smaczniak, C., Krajewski, P., and Angenent, G.C. (2009). Target genes of the MADS transcription factor SEPALLATA3: integration of developmental and hormonal pathways in the Arabidopsis flower. PLoS Biol **7,** e1000090.

Kempin, S.A., Savidge, B., and Yanofsky, M.F. (1995). Molecular basis of the cauliflower phenotype in Arabidopsis. Science **267,** 522-525.

Kobayashi, K., Maekawa, M., Miyao, A., Hirochika, H., and Kyozuka, J. (2010). PANICLE PHYTOMER2 (PAP2), encoding a SEPALLATA subfamily MADS-box protein, positively controls spikelet meristem identity in rice. Plant Cell Physiol **51,** 47-57.

Kobayashi, K., Yasuno, N., Sato, Y., Yoda, M., Yamazaki, R., Kimizu, M., Yoshida, H., Nagamura, Y., and Kyozuka, J. (2012). Inflorescence meristem identity in rice is specified by overlapping functions of three AP1/FUL-like MADS box genes and PAP2, a SEPALLATA MADS box gene. Plant Cell **24,** 1848-1859.

Koes, R., Souer, E., van Houwelingen, A., Mur, L., Spelt, C., Quattrocchio, F., Wing, J., Oppedijk, B., Ahmed, S., Maes, T., and et al. (1995). Targeted gene inactivation in petunia by PCR-based selection of transposon insertion mutants. Proc Natl Acad Sci U S A **92,** 8149-8153.

Koo, S.C., Bracko, O., Park, M.S., Schwab, R., Chun, H.J., Park, K.M., Seo, J.S., Grbic, V., Balasubramanian, S., Schmid, M., Godard, F., Yun, D.J., Lee, S.Y., Cho, M.J., Weigel, D., and Kim, M.C. (2010). Control of lateral organ development and flowering time by the Arabidopsis thaliana MADS-box Gene AGAMOUS-LIKE6. Plant J **62,** 807-816.

Krizek, B.A., and Fletcher, J.C. (2005). Molecular mechanisms of flower development: an armchair guide. Nat Rev Genet **6,** 688-698.

Lee, S., Kim, J., Son, J.S., Nam, J., Jeong, D.H., Lee, K., Jang, S., Yoo, J., Lee, J., Lee, D.Y., Kang, H.G., and An, G. (2003). Systematic reverse genetic screening of T-DNA tagged genes in rice for functional genomic analyses: MADS-box genes as a test case. Plant Cell Physiol **44,** 1403-1411.

Lemoine, F., Domelevo Entfellner, J.B., Wilkinson, E., Correia, D., Davila Felipe, M., De Oliveira, T., and Gascuel, O. (2018). Renewing Felsenstein's phylogenetic bootstrap in the era of big data. Nature **556,** 452-456.

Lemoine, F., Correia, D., Lefort, V., Doppelt-Azeroual, O., Mareuil, F., Cohen-Boulakia, S., and Gascuel, O. (2019). NGPhylogeny.fr: new generation phylogenetic services for non-specialists. Nucleic Acids Res **47,** W260-W265.

Leseberg, C.H., Eissler, C.L., Wang, X., Johns, M.A., Duvall, M.R., and Mao, L. (2008). Interaction study of MADS-domain proteins in tomato. J Exp Bot **59,** 2253-2265.

Litt, A. (2007). An Evaluation of A-Function: Evidence from the *APETALA1* and *APETALA2* Gene Lineages. International Journal of Plant Sciences **168,** 73-91.

Litt, A., and Irish, V.F. (2003). Duplication and diversification in the APETALA1/FRUITFULL floral homeotic gene lineage: implications for the evolution of floral development. Genetics **165,** 821-833.

Liu, D., Wang, D., Qin, Z., Zhang, D., Yin, L., Wu, L., Colasanti, J., Li, A., and Mao, L. (2014). The SEPALLATA MADS-box protein SLMBP21 forms protein complexes with JOINTLESS and MACROCALYX as a transcription activator for development of the tomato flower abscission zone. Plant J **77,** 284-296.

Maheepala, D.C., Emerling, C.A., Rajewski, A., Macon, J., Strahl, M., Pabon-Mora, N., and Litt, A. (2019). Evolution and Diversification of FRUITFULL Genes in Solanaceae. Front Plant Sci **10,** 43.

Malcomber, S.T., and Kellogg, E.A. (2005). SEPALLATA gene diversification: brave new whorls. Trends Plant Sci **10,** 427-435.

Mandel, M.A., Gustafson-Brown, C., Savidge, B., and Yanofsky, M.F. (1992). Molecular characterization of the Arabidopsis floral homeotic gene APETALA1. Nature **360,** 273-277.

McCarthy, E.W., Mohamed, A., and Litt, A. (2015). Functional Divergence of APETALA1 and FRUITFULL is due to Changes in both Regulation and Coding Sequence. Front Plant Sci **6,** 1076.

Melzer, R., Verelst, W., and Theissen, G. (2009). The class E floral homeotic protein SEPALLATA3 is sufficient to loop DNA in 'floral quartet'-like complexes in vitro. Nucleic Acids Res **37,** 144-157.

Monniaux, M., and Vandenbussche, M. (2018). How to Evolve a Perianth: A Review of Cadastral Mechanisms for Perianth Identity. Front Plant Sci **9,** 1573.

Moore, M.J., Soltis, P.S., Bell, C.D., Burleigh, J.G., and Soltis, D.E. (2010). Phylogenetic analysis of 83 plastid genes further resolves the early diversification of eudicots. Proceedings of the National Academy of Sciences **107,** 4623-4628.

Morel, P., Heijmans, K., Ament, K., Chopy, M., Trehin, C., Chambrier, P., Rodrigues Bento, S., Bimbo, A., and Vandenbussche, M. (2018). The Floral C-Lineage Genes Trigger Nectary Development in Petunia and Arabidopsis. Plant Cell **30,** 2020-2037.

Morel, P., Heijmans, K., Rozier, F., Zethof, J., Chamot, S., Bento, S.R., Vialette-Guiraud, A., Chambrier, P., Trehin, C., and Vandenbussche, M. (2017). Divergence of the

Floral A-Function between an Asterid and a Rosid Species. Plant Cell **29,** 1605-1621.

Nakano, T., Kimbara, J., Fujisawa, M., Kitagawa, M., Ihashi, N., Maeda, H., Kasumi, T., and Ito, Y. (2012). MACROCALYX and JOINTLESS interact in the transcriptional regulation of tomato fruit abscission zone development. Plant Physiol **158,** 439-450.

Ohmori, S., Kimizu, M., Sugita, M., Miyao, A., Hirochika, H., Uchida, E., Nagato, Y., and Yoshida, H. (2009). MOSAIC FLORAL ORGANS1, an AGL6-like MADS box gene, regulates floral organ identity and meristem fate in rice. Plant Cell **21,** 3008-3025.

OMaoileidigh, D.S., Wuest, S.E., Rae, L., Raganelli, A., Ryan, P.T., Kwasniewska, K., Das, P., Lohan, A.J., Loftus, B., Graciet, E., and Wellmer, F. (2013). Control of reproductive floral organ identity specification in Arabidopsis by the C function regulator AGAMOUS. Plant Cell **25,** 2482-2503.

Park, S.J., Eshed, Y., and Lippman, Z.B. (2014). Meristem maturation and inflorescence architecture–lessons from the Solanaceae. Curr Opin Plant Biol **17,** 70-77.

Pelaz, S., Ditta, G.S., Baumann, E., Wisman, E., and Yanofsky, M.F. (2000). B and C floral organ identity functions require SEPALLATA MADS-box genes. Nature **405,** 200-203.

Pelaz, S., Gustafson-Brown, C., Kohalmi, S.E., Crosby, W.L., and Yanofsky, M.F. (2001). APETALA1 and SEPALLATA3 interact to promote flower development. Plant J **26,** 385-394.

Pnueli, L., Hareven, D., Broday, L., Hurwitz, C., and Lifschitz, E. (1994). The TM5 MADS Box Gene Mediates Organ Differentiation in the Three Inner Whorls of Tomato Flowers. Plant Cell **6,** 175-186.

Purugganan, M.D. (1997). The MADS-box floral homeotic gene lineages predate the origin of seed plants: phylogenetic and molecular clock estimates. J Mol Evol **45,** 392-396.

Purugganan, M.D., Rounsley, S.D., Schmidt, R.J., and Yanofsky, M.F. (1995). Molecular evolution of flower development: diversification of the plant MADS-box regulatory gene family. Genetics **140,** 345-356.

Rijpkema, A.S., Zethof, J., Gerats, T., and Vandenbussche, M. (2009). The petunia AGL6 gene has a SEPALLATA-like function in floral patterning. Plant J **60,** 1-9.

Rijpkema, A.S., Royaert, S., Zethof, J., van der Weerden, G., Gerats, T., and Vandenbussche, M. (2006). Analysis of the *Petunia TM6* MADS box gene reveals functional divergence within the *DEF*/*AP3* lineage. Plant Cell **18,** 1819-1832.

Roldan, M.V.G., Perilleux, C., Morin, H., Huerga-Fernandez, S., Latrasse, D., Benhamed, M., and Bendahmane, A. (2017). Natural and induced loss of function mutations in SlMBP21 MADS-box gene led to jointless-2 phenotype in tomato. Sci Rep **7,** 4402.

Shima, Y., Kitagawa, M., Fujisawa, M., Nakano, T., Kato, H., Kimbara, J., Kasumi, T., and Ito, Y. (2013). Tomato FRUITFULL homologues act in fruit ripening via forming MADS-box transcription factor complexes with RIN. Plant Mol Biol **82,** 427-438.

Souer, E., Rebocho, A.B., Bliek, M., Kusters, E., de Bruin, R.A., and Koes, R. (2008). Patterning of inflorescences and flowers by the F-Box protein DOUBLE TOP and the LEAFY homolog ABERRANT LEAF AND FLOWER of petunia. Plant Cell **20,** 2033-2048.

Souer, E., van der Krol, A., Kloos, D., Spelt, C., Bliek, M., Mol, J., and Koes, R. (1998). Genetic control of branching pattern and floral identity during Petunia inflorescence development. Development **125,** 733-742.

Soyk, S., Lemmon, Z.H., Oved, M., Fisher, J., Liberatore, K.L., Park, S.J., Goren, A., Jiang, K., Ramos, A., van der Knaap, E., Van Eck, J., Zamir, D., Eshed, Y., and Lippman, Z.B. (2017). Bypassing Negative Epistasis on Yield in Tomato Imposed by a Domestication Gene. Cell **169,** 1142-1155 e1112.

Stam, M., Mol, J.N.M., and Kooter, J.M. (1997). The silence of genes in transgenic plants. Ann Bot **79,** 3-12.

Taylor, S.A., Hofer, J.M., Murfet, I.C., Sollinger, J.D., Singer, S.R., Knox, M.R., and Ellis, T.H. (2002). PROLIFERATING INFLORESCENCE MERISTEM, a MADS-box gene that regulates floral meristem identity in pea. Plant Physiol **129,** 1150-1159.

The Tomato Genome Consortium. (2012). The tomato genome sequence provides insights into fleshy fruit evolution. Nature **485,** 635-641.

Theissen, G., and Saedler, H. (2001). Plant biology. Floral quartets. Nature **409,** 469-471.

Thompson, B.E., Bartling, L., Whipple, C., Hall, D.H., Sakai, H., Schmidt, R., and Hake, S. (2009). bearded-ear encodes a MADS box transcription factor critical for maize floral development. Plant Cell **21,** 2578-2590.

van der Krol, A.R., Brunelle, A., Tsuchimoto, S., and Chua, N.H. (1993). Functional analysis of petunia floral homeotic MADS box gene pMADS1. Genes Dev **7,** 1214-1228.

Vandenbussche, M., Theissen, G., Van de Peer, Y., and Gerats, T. (2003a). Structural diversification and neo-functionalization during floral MADS-box gene evolution by C-terminal frameshift mutations. Nucleic Acids Res **31,** 4401-4409.

Vandenbussche, M., Chambrier, P., Rodrigues Bento, S., and Morel, P. (2016). Petunia, Your Next Supermodel? Front Plant Sci **7,** 72.

Vandenbussche, M., Zethof, J., Royaert, S., Weterings, K., and Gerats, T. (2004). The duplicated B-class heterodimer model: whorl-specific effects and complex genetic interactions in *Petunia hybrida* flower development. Plant Cell **16,** 741-754.

Vandenbussche, M., Horstman, A., Zethof, J., Koes, R., Rijpkema, A.S., and Gerats, T. (2009). Differential recruitment of WOX transcription factors for lateral development and organ fusion in Petunia and Arabidopsis. Plant Cell **21,** 2269-2283.

Vandenbussche, M., Zethof, J., Souer, E., Koes, R., Tornielli, G.B., Pezzotti, M., Ferrario, S., Angenent, G.C., and Gerats, T. (2003b). Toward the analysis of the petunia MADS box gene family by reverse and forward transposon insertion mutagenesis approaches: B, C, and D floral organ identity functions require SEPALLATA-like MADS box genes in petunia. Plant Cell **15,** 2680-2693.

Vandenbussche, M., Janssen, A., Zethof, J., van Orsouw, N., Peters, J., van Eijk, M.J., Rijpkema, A.S., Schneiders, H., Santhanam, P., de Been, M., van Tunen, A., and Gerats, T. (2008). Generation of a 3D indexed Petunia insertion database for reverse genetics. Plant J **54,** 1105-1114.

Vrebalov, J., Ruezinsky, D., Padmanabhan, V., White, R., Medrano, D., Drake, R., Schuch, W., and Giovannoni, J. (2002). A MADS-box gene necessary for fruit ripening at the tomato ripening-inhibitor (rin) locus. Science **296,** 343-346.

Wang, S., Lu, G., Hou, Z., Luo, Z., Wang, T., Li, H., Zhang, J., and Ye, Z. (2014). Members of the tomato FRUITFULL MADS-box family regulate style abscission and fruit ripening. J Exp Bot **65,** 3005-3014.

Weigel, D., Alvarez, J., Smyth, D.R., Yanofsky, M.F., and Meyerowitz, E.M. (1992). LEAFY controls floral meristem identity in Arabidopsis. Cell **69,** 843-859.

Wu, D., Liang, W., Zhu, W., Chen, M., Ferrandiz, C., Burton, R.A., Dreni, L., and Zhang, D. (2017a). Loss of LOFSEP transcription factor function converts Spikelet to Leaf-like Structures in Rice. Plant Physiol.

Wu, F., Shi, X., Lin, X., Liu, Y., Chong, K., Theissen, G., and Meng, Z. (2017b). The ABCs of flower development: mutational analysis of AP1/FUL-like genes in rice provides evidence for a homeotic (A)-function in grasses. Plant J **89,** 310-324.

Yu, H., Ito, T., Wellmer, F., and Meyerowitz, E.M. (2004). Repression of AGAMOUS-LIKE 24 is a crucial step in promoting flower development. Nature Genetics **36,** 157-161.

Yu, X., Duan, X., Zhang, R., Fu, X., Ye, L., Kong, H., Xu, G., and Shan, H. (2016). Prevalent Exon-Intron Structural Changes in the APETALA1/FRUITFULL, SEPALLATA, AGAMOUS-LIKE6, and FLOWERING LOCUS C MADS-Box Gene Subfamilies Provide New Insights into Their Evolution. Front Plant Sci **7,** 598.

Yu, X., Chen, G., Guo, X., Lu, Y., Zhang, J., Hu, J., Tian, S., and Hu, Z. (2017). Silencing SlAGL6, a tomato AGAMOUS-LIKE6 lineage gene, generates fused sepal and green petal. Plant Cell Rep **36,** 959-969.

Yuste-Lisbona, F.J., Quinet, M., Fernandez-Lozano, A., Pineda, B., Moreno, V., Angosto, T., and Lozano, R. (2016). Characterization of vegetative inflorescence (mc-vin) mutant provides new insight into the role of MACROCALYX in regulating inflorescence development of tomato. Sci Rep **6,** 18796.

Zahn, L.M., Kong, H., Leebens-Mack, J.H., Kim, S., Soltis, P.S., Landherr, L.L., Soltis, D.E., Depamphilis, C.W., and Ma, H. (2005). The evolution of the SEPALLATA subfamily of MADS-box genes: a preangiosperm origin with multiple duplications throughout angiosperm history. Genetics **169,** 2209-2223.

FIGURE LEGENDS

Figure 1. Characterization of the Petunia *SEP/AGL6* MADS-box Genes.

(A) Section through a WT petunia W138 flower showing inner whorls. **(B)** Petunia seedpod ~4 weeks post-pollination surrounded by green sepals. **(C)** SEM (scanning electron microscopy) images of sepal, bract and leaf adaxial and abaxial epidermal surfaces. Bars = 50 µm. **(D)** Longitudinal sections of developing petunia floral buds showing the placenta developing from the center of the floral meristem s = sepal; p = petal; st = stamen; c = carpel; pl = placenta. Bars = 200 µm. **(E)** W138 floral bud developmental stages for RT-qPCR analysis shown in (G), dissected from the top of an inflorescence (inset), of which the large floral bud at the right is just prior to opening. Numbers indicate sampled stages. 1 to 3 correspond to floral bud diameters of ~1.5, 2.5 and 5 mm respectively. Stage 1 also includes very early flower primordia, bracts and the inflorescence meristem. Bar = 1 cm. **(F)** Maximum Likelihood phylogenetic analysis of the SEP and AGL6 subfamily members of *Petunia hybrida* (*Ph*), *Solanum lycopersicum* (*Sl*), *Arabidopsis thaliana* (*At*) and *Oryza sativa* (*Os*). Bootstrap values marked in red (expressed in %, based on 1000 replicates) supporting tree branching are indicated near

the branching points. The scale bar represents number of substitutions per site. Accession codes for the corresponding sequences are shown in Supplemental Table 1. Naming of subfamilies and subfamily clades is based on previously described phylogenies for the SEP subfamily (Malcomber and Kellogg, 2005; Zahn et al., 2005; Yu et al., 2016). **(G)** RT-qPCR expression analysis of the petunia *SEP/AGL6* genes. Relative expression (R.E.) levels are plotted as the mean value of three biological and three technical replicates ±SE, normalized against three reference genes (see Material and Methods). Expression levels were measured in vegetative tissues (green bars; infl. stem = inflorescence stem); entire floral buds (orange bars) from 3 developmental stages shown in (E) and dissected floral organs (red bars) obtained from flower buds corresponding to stage 3. **(H)** Schematic representations of the gene structures and insertion alleles of the petunia *SEP and AGL6* genes and floral phenotypes of the corresponding insertion mutants used in further crosses. Black boxes and lines represent exons and introns respectively. All gene models start at the start codon and end at the stop codon. Scale bars = 500 bp. Red triangles indicate positions of *dTph1* transposon insertions. Alleles are named after the exact insert position of the *dTph1* element in number of base pairs downstream of the ATG in the coding sequence. The names of the insertion alleles that have been selected for the creation of double and higher order mutants are marked in red.

Figure 2. The Petunia *fbp2 fbp5 pm12* Mutant, Genetic Equivalent of the Arabidopsis *sep1 sep2 sep3* Mutant, Still Displays B- and C-function Floral Characteristics.

(A) to **(H)** Top view of flowers from WT, single, double and triple mutants of petunia *SEP1*/*SEP2*/*SEP3* homologs. All images are at the same magnification. **(I)** to **(L)** Side view of WT and mutant flowers sectioned through the middle. All images are at the same magnification. **(M)** Close-up of dissected third whorl organs (stamens). **(N)** Close-up of dissected fourth whorl organs (carpels). **(O)** to **(Q)** SEM images of the outer ovary surface. Scale bars = 100 µm.

Figure 3. Petunia Floral Meristem Identity Depends on *FBP9*/*FBP23*/*FBP4* Activity.

(A) to **(C)** and **(E)** to **(G)** Top and side view of *WT*, *fbp9 fbp23* and *fbp9 fbp23 fbp4* plants 13 weeks after sowing. **(D)** and **(H)** Schematic representation of inflorescence phenotypes. **(I)** to **(L)** SEM images of inflorescence apices in *WT* and *fbp4 fbp9 fbp23* mutants. Br: bracts; Se: sepals; F: flower; Fm: Flower meristem; Im: Inflorescence meristem. Scale bars = 100 µm. **(M)** to **(Q)** Inflorescence architecture of lower order mutants compared to WT and *fbp9 fbp23 fbp4* mutants. **(R)** to **(W)** Flower phenotypes of *fbp4*, *fbp23* and *fbp9* mutations in combination with *fbp2*. All flowers are at the same magnification.

Figure 4. Characterization of the Sextuple *fbp2 fbp4 fbp5 fbp9 pm12 agl6* Mutant Compared to WT. Genotypes in each panel are indicated as follows: sext: sextuple *fbp2 fbp4 fbp5 fbp9 pm12 agl6* mutant. WT: wild-type.

(A) and **(B)** Top view of young (A) and mature flower (B). **(C)** Dissected floral organs of a flower similar to the stage as indicated by the asterisk in (F). W# indicate whorl numbers. **(D)** Longitudinal section through an older flower similar to the stage as indicated by the double asterisk in (F). **(E)** SEM images of the epidermis of the four different floral whorls (indicated by W#) in WT (left panels) and the sextuple mutant (right panels). **(F)** Inflorescences showing flowers at various stages of development and aging. The arrows indicate an example where three consecutive fully developed flowers arose from a single floral meristem. Scale bars: 0.25 cm in (A); 0.5 cm in (B, D); 1 cm in (C, F); 50 µm in (E). **(G)** RT-qPCR expression analysis of the petunia floral homeotic genes in WT versus sextuple *fbp2 fbp4 fbp5 fbp9 pm12 agl6* mutants**.** Petunia genes are indicated and names of corresponding Arabidopsis orthologs are shown in between brackets. *No *TM6* ortholog exists in the Arabidopsis genome. **Petunia *FBP6* is orthologous to *SHP1*/*SHP2*, but is functionally homologous to *AG*. Relative expression (R.E.) levels are plotted as the mean value of three biological and three technical replicates ±SE, normalized against three reference genes (see Material and Methods). Expression levels were measured in entire floral buds from three developmental stages as shown in Figure 1E.

Figure 5. Characterization of the Petunia AP1/SQUA MADS-box Subfamily.

(A) Maximum likelihood phylogenetic analysis of the AP1/SQUA subfamily members of *Petunia hybrida (Ph)*, *Solanum lycopersicum (Sl)*, *Arabidopsis thaliana (At)* and *Oryza sativa (Os)*. Bootstrap values marked in red (expressed in %, based on 1000 replicates) supporting branching are indicated near the branch points. The scale bar represents number of substitutions/site. Accession codes for the corresponding sequences are shown in Supplemental Table 1. Naming of subfamilies and subfamily clades is based on previously described phylogenies for the AP1/SQUA subfamily (Litt and Irish, 2003; Yu et al., 2016; Maheepala et al., 2019). **(B)** RT-qPCR expression analysis of the petunia *AP1/SQUA* genes. Relative expression (R.E.) levels are plotted as the mean value of three biological and three technical replicates ±SE, normalized against three reference genes (see Material and Methods). See legend of Figure 1G for sample description. **(C)** Schematic representations of the gene structures and insertion alleles of the petunia *AP1/SQUA* genes and corresponding floral

phenotypes of insertion lines used for further crosses and analyses. Figure Legend as in Figure 1H.

Figure 6. Petunia *AP1/SQUA* Family Members are Required for Inflorescence Meristem Identity and Repress the B-function in the First Floral Whorl.

(A) to **(D)** Flower phenotype of *pfg fbp26 fbp29 euap1* mutants. Some sepals and petals have been removed in (B) to reveal inner organs. **(D)** Enlarged sepals showing petaloid sectors displaying petal conical epidermal cells (inset SEM image). **(E)** to **(G)** Inflorescence phenotype showing an "inflorescence" with spirally organized leaves (F) ending in a single terminal flower (G). **(L)** Side branches developing from the basis of the plant exhibit an identical inflorescence phenotype. **(H), (I)** and **(M)** Longitudinal sections of the apex of an inflorescence in vegetative state (G), and of an inflorescence with terminal flower (I), compared to the apex of a WT inflorescence (M). Red asterisks in (I) indicate vegetative lateral meristems. **(J)** to **(K)** Enhanced homeotic sepal-to-petal conversion compared to (C) and (D). **(N)** and **(O)** unmodified sepals in *rob1 rob2/+ rob3* mutants (N) compared to WT (O). **(P)** and **(Q)** SEM images of a WT vegetative meristem before the onset to flowering compared to the apex of a *pfg fbp26 fbp29 euap1* inflorescence prior to terminal flower formation as in (H). **(R)** Schematic representation of a *pfg fbp26 fbp29 euap1* inflorescence (right) compared to an intermediate inflorescence phenotype as shown in (T) to (V). **(S)** to **(X)** Inflorescence phenotypes of WT, quadruple and various triple mutant combinations after prolonged flowering. White arrows indicate positions of previous terminal flowers. Scale bars: 1 cm in (A-G; J-L; N-O; S-X); 100 µm in (P-Q; H, I, M); 50 µm in inset in (D).

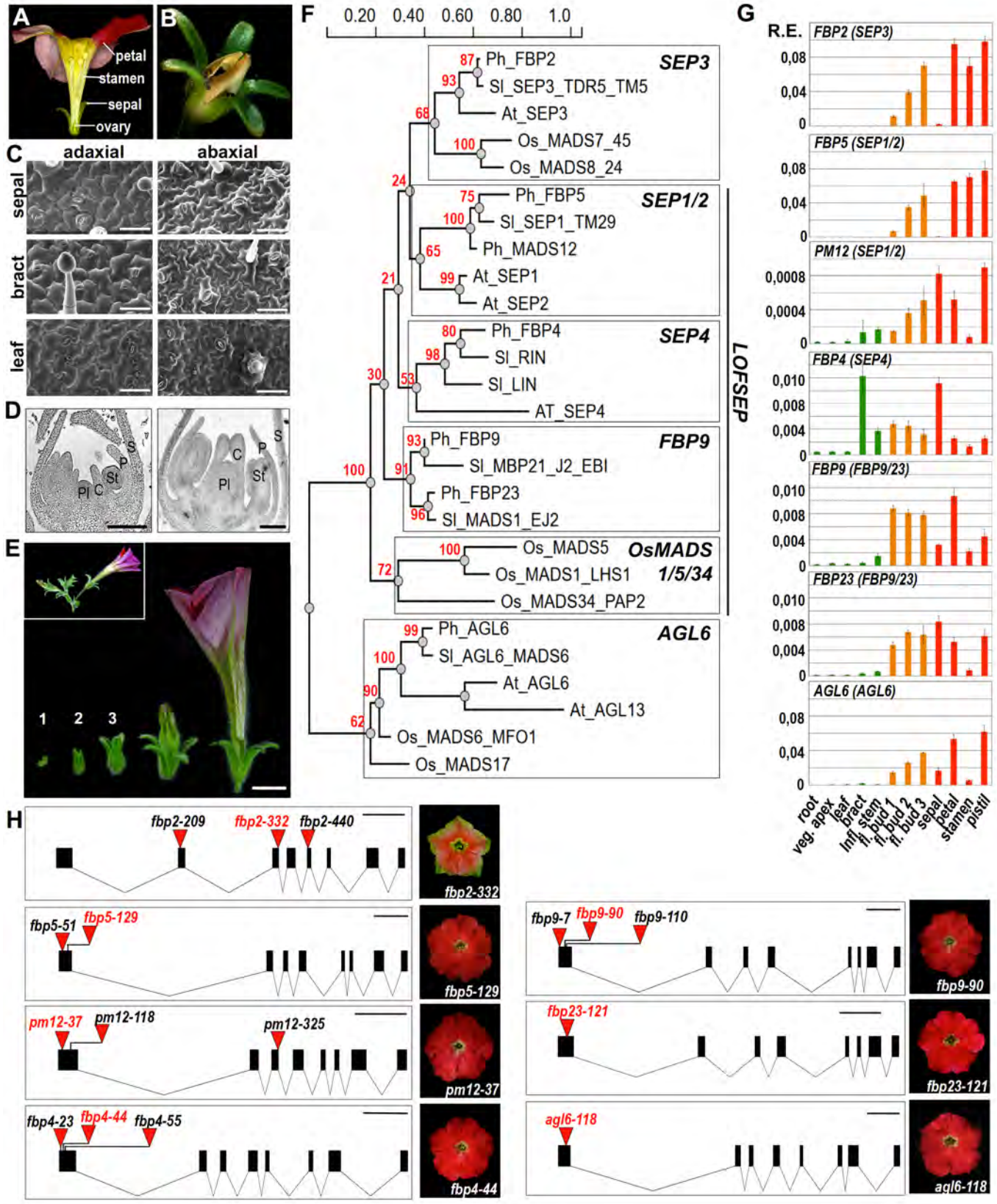

Figure 1. Characterization of the Petunia *SEP/AGL6* MADS-box Genes.

(A) Section through a WT petunia W138 flower showing inner whorls. (B) Petunia seedpod ~4 weeks post-pollination surrounded by green sepals. (C) SEM (scanning electron microscopy) images of sepal, bract and leaf adaxial and abaxial epidermal surfaces. Bars = 50 µm. (D) Longitudinal sections of developing petunia floral buds showing the placenta developing from the center of the floral meristem s = sepal; p = petal; st = stamen; c = carpel; pl = placenta. Bars = 200 µm. (E) W138 floral bud developmental stages for RT-qPCR analysis shown in (G), dissected from the top of an inflorescence (inset), of which the large floral bud at the right is just prior to opening. Numbers indicate sampled stages. 1 to 3 correspond to floral bud diameters of ~1.5; 2.5 and 5 mm respectively. Stage 1 includes also very early flower primordia, bracts and the inflorescence meristem. Bar = 1 cm. (F) Maximum Likelyhood phylogenetic analysis of the SEP and AGL6 subfamily members of *Petunia hybrida (Ph), Solanum lycopersicum (Sl), Arabidopsis thaliana (At)* and *Oryza sativa (Os)*. Bootstrap values marked in red (expressed in %, based on 1000 replicates) supporting tree branching are indicated near the branching points. The scalebar represents number of substitutions/site. Accession codes for the corresponding sequences are shown in Supplemental Table 1. Naming of subfamilies and subfamily clades are based on previously described phylogenies for the SEP subfamily (Malcomber and Kellogg, 2005; Zahn et al., 2005; Yu et al., 2016). (G) RT-qPCR expression analysis of the petunia *SEP/AGL6* genes. Relative expression (R.E.) levels are plotted as the mean value of three biological and three technical replicates ±SE, normalized against three reference genes (see Material and Methods). Expression levels were measured in vegetative tissues (green bars; infl. stem = inflorescence stem); entire floral buds (orange bars) from 3 developmental stages shown in (E) and dissected floral organs (red bars) obtained from flower buds corresponding to stage 3. (H) Schematic representations of the gene structures and insertion alleles of the petunia *SEP and AGL6* genes and floral phenotypes of the corresponding insertion mutants used in further crosses. Black boxes and lines represent exons and introns respectively. All gene models start at the start codon and end at the stop codon. Scale Bars = 500 bp. Red triangles indicate positions of *dTph1* transposon insertions. Alleles are named after the exact insert position of the *dTph1* element in number of basepairs downstream of the ATG in the coding sequence. The names of the insertion alleles that have been selected for the creation of double and higher order mutants are marked in red.

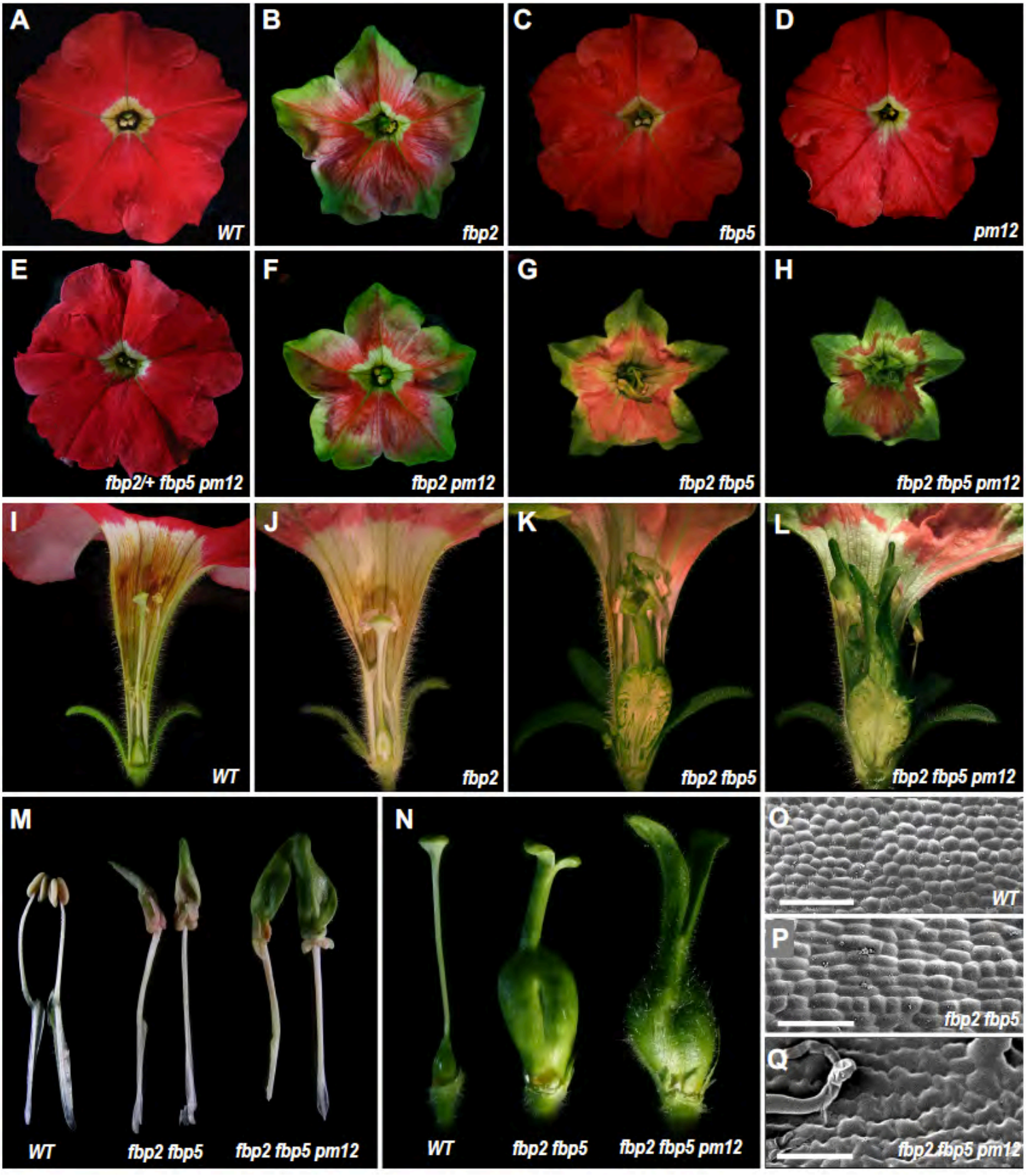

Figure 2. The Petunia *fbp2 fbp5 pm12* Mutant, Genetic Equivalent of the Arabidopsis *sep1 sep2 sep3* Mutant Still Displays B- and C-function Floral Characteristics. (A) to (H) Topview of flowers from WT, single, double and triple mutants of petunia *SEP1/2/3* homologs. All images are at the same magnification. (I) to (L) Sideview of WT and mutant flowers sectioned through the middle. All images are at the same magnification. (M) Close-up of dissected third whorl organs (stamens). (N) Close-up of dissected fourth whorl organs (carpels). (O) to (Q) SEM images of the outer ovary surface. Scale bars = 100 μm.

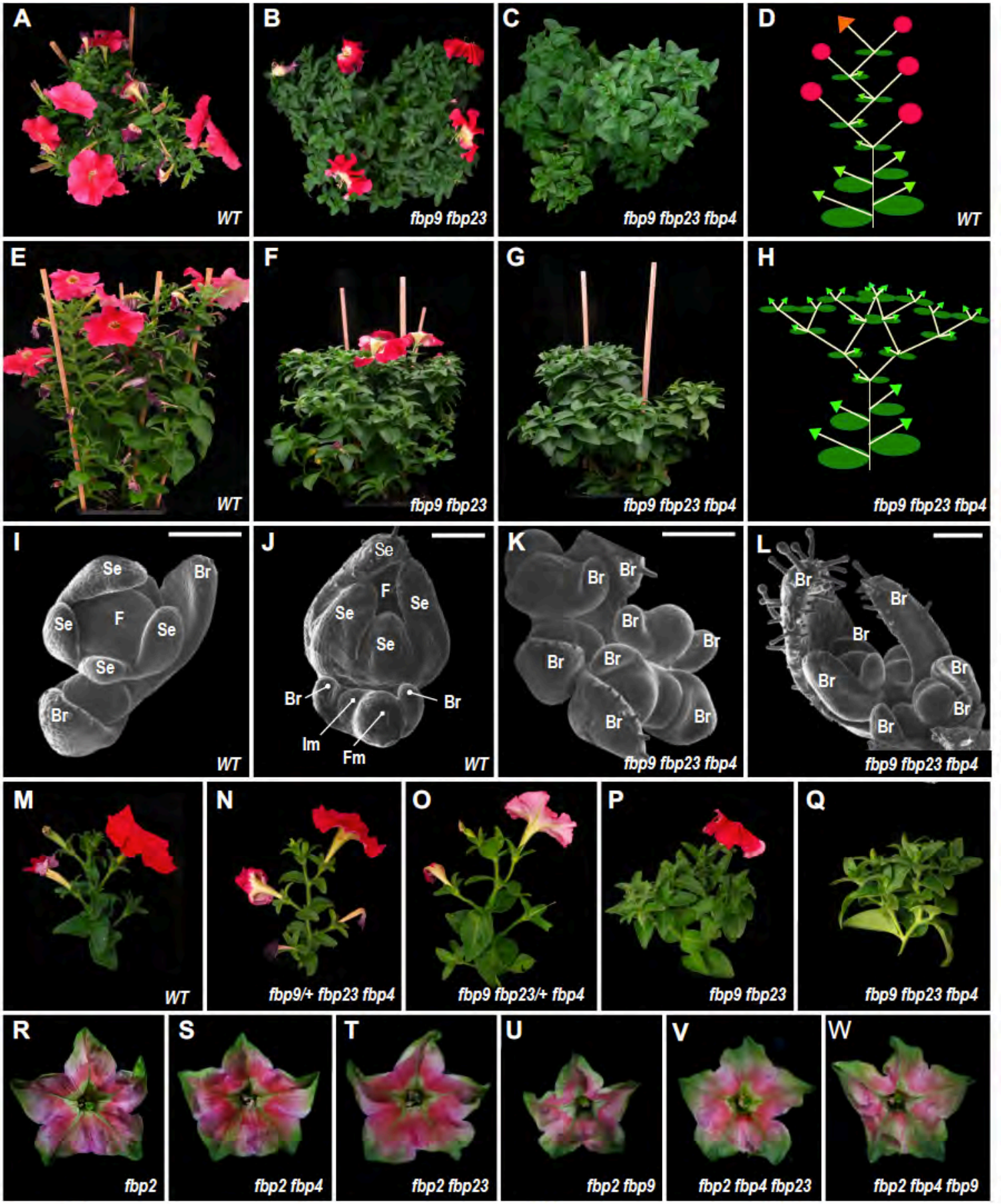

Figure 3. Petunia Floral Meristem Identity Depends on *FBP9/23/4* Activity.
(A) to (C) and (E) to (G) Top- and side view of *WT*, *fbp9 fbp23* and *fbp9 fbp23 fbp4* plants 13 weeks after sowing. (D) and (H) Schematic representation of inflorescence phenotypes. (I) to (L) SEM images of inflorescence apices in *WT* and *fbp4 fbp9 fbp23* mutants. Br: bracts; Se: sepals; F: flower; Fm: Flower meristem; Im: Inflorescence meristem. Scale bars = 100 µm. (M) to (Q) Inflorescence architecture of lower order mutants compared to WT and *fbp9 fbp23 fbp4* mutants. (R) to (W) Flower phenotypes of *fbp4*, *fbp23* and *fbp9* mutations in combination with *fbp2*. All flowers are at the same magnification.

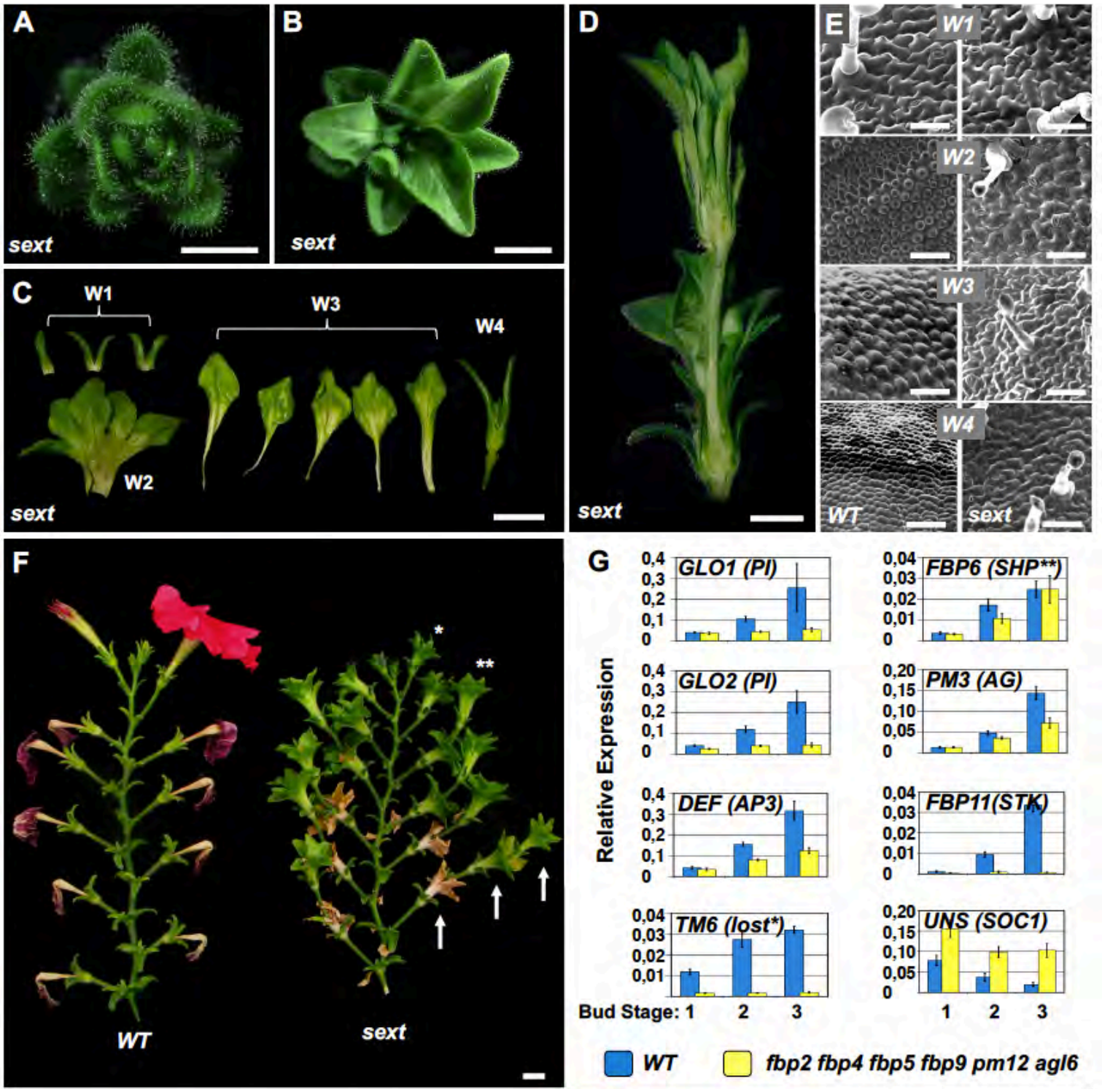

Figure 4. Characterization of the Sextuple *fbp2 fbp4 fbp5 fbp9 pm12 agl6* Mutant compared to WT. Genotypes in each panel are indicated as follows: sext: sextuple *fbp2 fbp4 fbp5 fbp9 pm12 agl6* mutant. WT: wild-type.

(A) and (B) Topview of young (A) and mature flower (B). (C) Dissected floral organs of a flower similar to the stage as indicated by the asterisk in (F). W# indicate whorl numbers. (D) Longitudinal section through an older flower similar to the stage as indicated by the double asterisk in (F). (E) SEM images of the epidermis of the four different floral whorls (indicated by W#) in WT (left panels) and the sextuple mutant (right panels). (F) Inflorescences showing flowers at various stages of development and aging. The arrows indicate an example where three consecutive fully developed flowers arose from a single floral meristem. Scalebars: 0,25 cm in (A); 0,5 cm in (B, D); 1cm in (C, F); 50 µm in (E). (G) RT-qPCR expression analysis of the petunia floral homeotic genes in WT versus sextuple *fbp2 fbp4 fbp5 fbp9 pm12 agl6* mutants. Petunia genes are each time indicated and names of corresponding Arabidopsis orthologs are shown in between brackets. *No *TM6* ortholog exists in the Arabidopsis genome. **Petunia *FBP6* is orthologous to *SHP1/2*, but is functionally homologous to *AG*. Relative expression (R.E.) levels were plotted as the mean value of three biological and three technical replicates ±SE, normalized against three reference genes (see Material and Methods). Expression levels were measured in entire floral buds from three developmental stages as shown in Figure 1E.

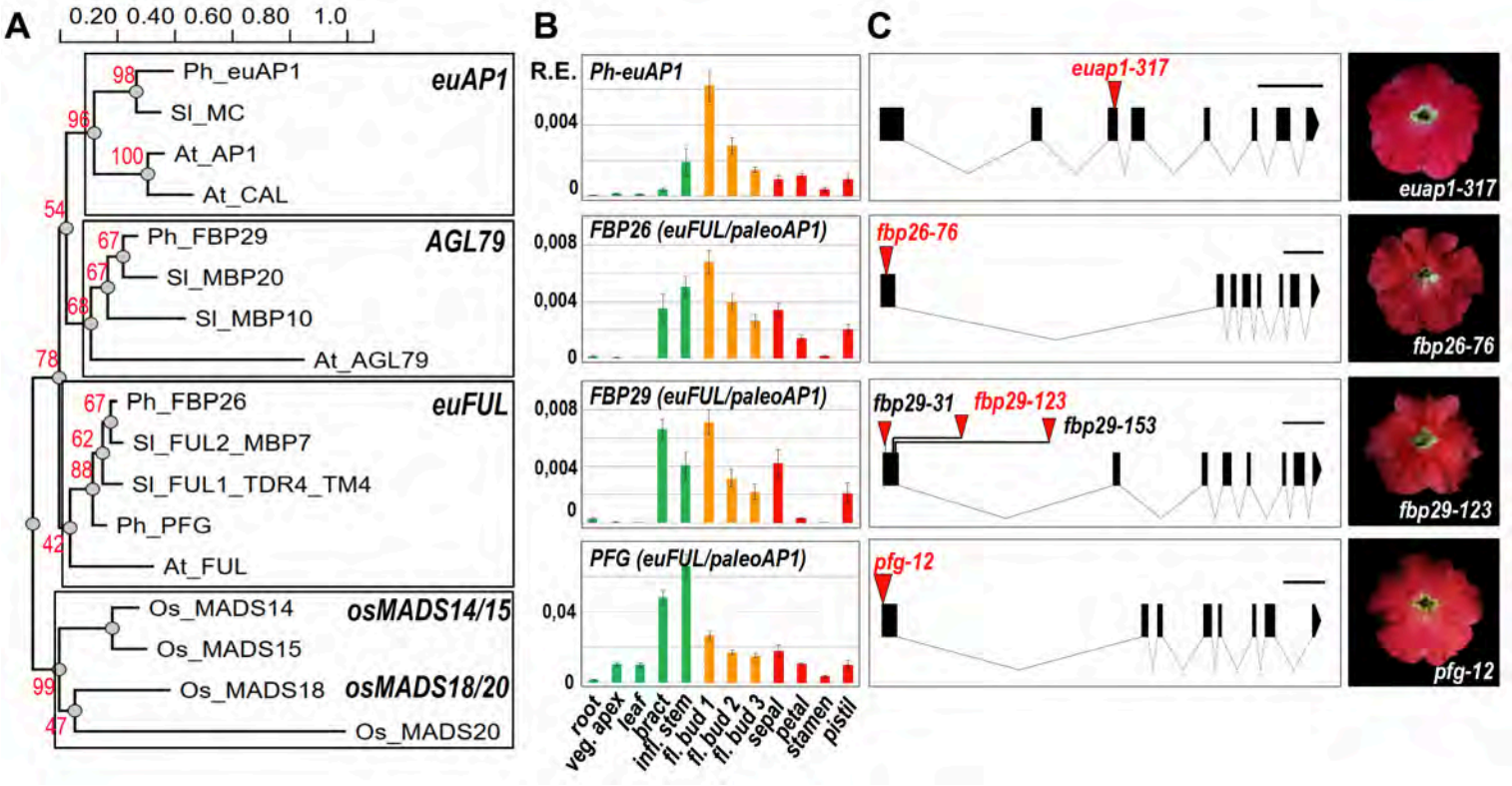

Figure 5. Characterization of the Petunia AP1/SQUA MADS-box Subfamily.

(A) Maximum Likelyhood phylogenetic analysis of the AP1/SQUA subfamily members of *Petunia hybrida (Ph), Solanum lycopersicum (Sl), Arabidopsis thaliana (At)* and *Oryza sativa (Os)*. Bootstrap values marked in red (expressed in %, based on 1000 replicates) supporting tree branching are indicated near the branching points. The scalebar represents number of substitutions/site. Accession codes for the corresponding sequences are shown in Supplemental Table 1. Naming of subfamilies and subfamily clades are based on previously described phylogenies for the AP1/SQUA subfamily (Litt and Irish, 2003; Yu et al., 2016; Maheepala et al., 2019). (B) RT-qPCR expression analysis of the petunia *AP1/SQUA* genes. Relative expression (R.E.) levels are plotted as the mean value of three biological and three technical replicates ±SE, normalized against three reference genes (see Material and Methods). See legend of Figure 1G for sample description. (C) Schematic representations of the gene structures and insertion alleles of the petunia *AP1/SQUA* genes and corresponding floral phenotypes of insertion lines used for further crosses and analyses. Figure Legend as in Figure 1H.

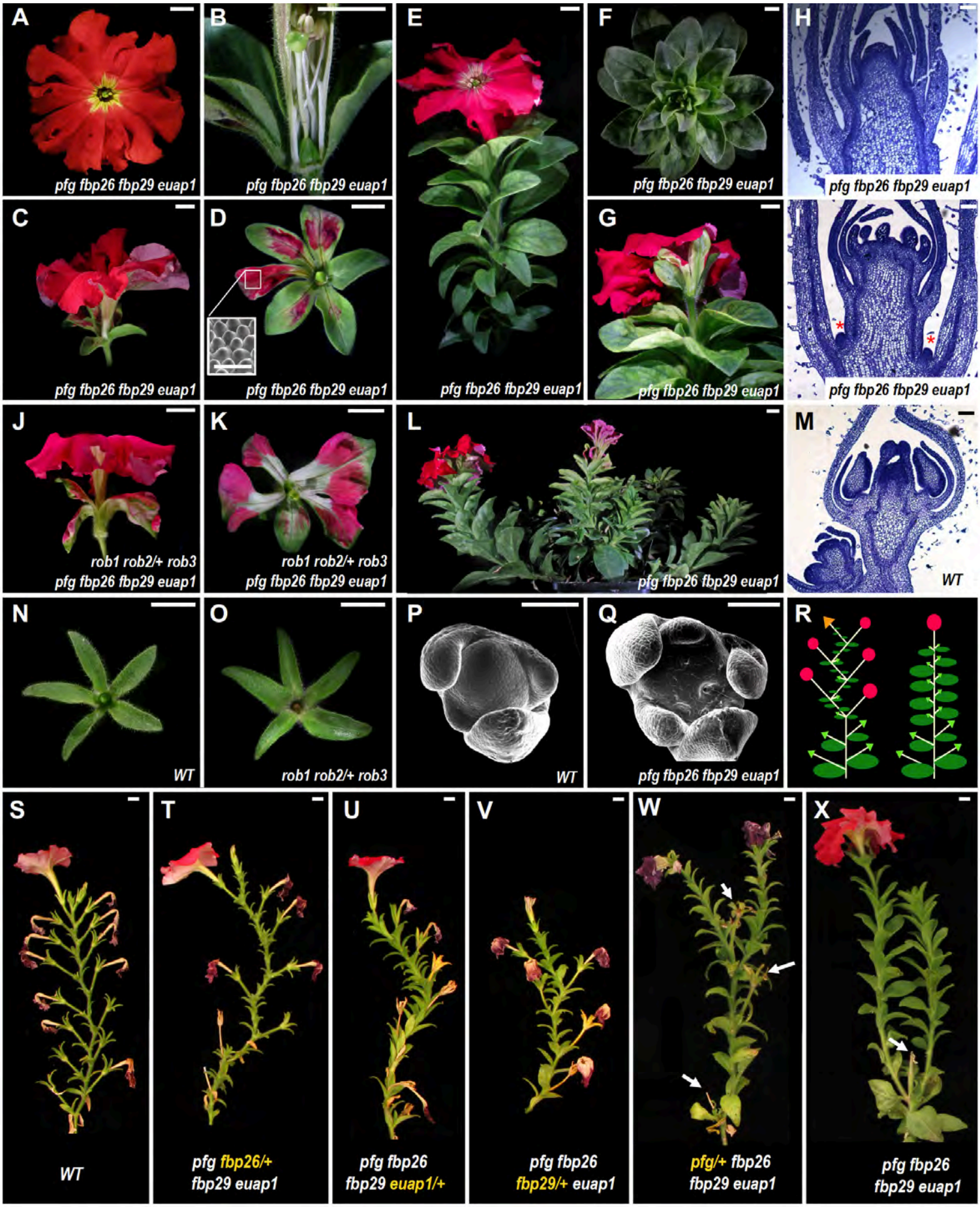

Figure 6. Petunia *AP1/SQUA* family members are Required for Inflorescence Meristem Identity, and Repress the B-function in the First Floral Whorl.
(A) to (D) Flower phenotype of *pfg fbp26 fbp29 euap1* mutants. Some sepals and petals have been removed in (B) to reveal inner organs. (D) Enlarged sepals showing petaloid sectors displaying petal conical epidermal cells (inset SEM image). (E) to (G) Inflorescence phenotype showing an "inflorescence" with spirally organized leaves (F) ending in a single terminal flower (G). (L) Side branches developing from the basis of the plant exhibit an identical inflorescence phenotype. (H), (I) and (M) Longitudinal sections of the apex of an inflorescence in vegetative state (G), and of an inflorescence with terminal flower (I), compared to the apex of a WT inflorescence (M). Red asterisks in (I) indicate vegetative lateral meristems. (J) to (K) Enhanced homeotic sepal-to-petal conversion compared to (C) and (D). (N) and (O) unmodified sepals in *rob1 rob2/+ rob3* mutants (N) compared to WT (O). (P) and (Q) SEM images of a WT vegetative meristem before the onset to flowering compared to the apex of a *pfg fbp26 fbp29 euap1* inflorescence prior to terminal flower formation as in (H). (R) Schematic representation of a *pfg fbp26 fbp29 euap1* inflorescence (right) compared to an intermediate inflorescence phenotype as shown in (T) to (V). (S) to (X) Inflorescence phenotypes of WT, quadruple and various triple mutant combinations after prolonged flowering. White arrows indicate positions of previous terminal flowers. Scale bars: 1 cm in (A-G; J-L; N-O; S-X); 100 µm in (P-Q; H, I, M); 50 µm in inset in (D).